

PCCP

Accepted Manuscript

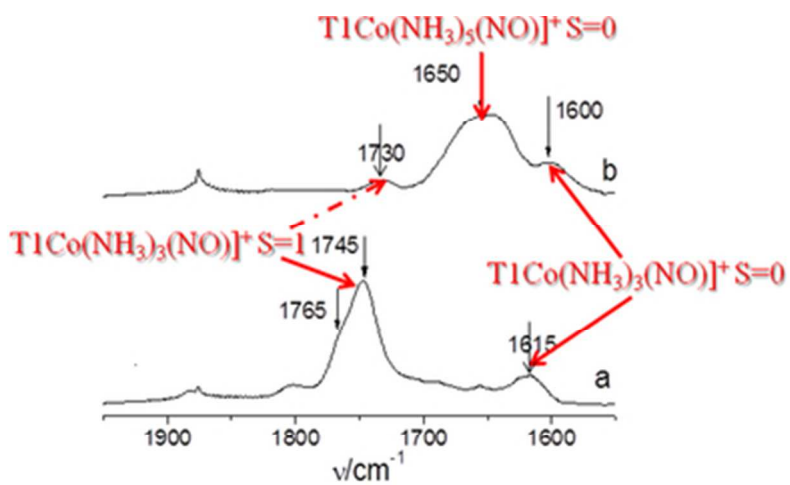


This is an *Accepted Manuscript*, which has been through the Royal Society of Chemistry peer review process and has been accepted for publication.

Accepted Manuscripts are published online shortly after acceptance, before technical editing, formatting and proof reading. Using this free service, authors can make their results available to the community, in citable form, before we publish the edited article. We will replace this *Accepted Manuscript* with the edited and formatted *Advance Article* as soon as it is available.

You can find more information about *Accepted Manuscripts* in the [Information for Authors](#).

Please note that technical editing may introduce minor changes to the text and/or graphics, which may alter content. The journal's standard [Terms & Conditions](#) and the [Ethical guidelines](#) still apply. In no event shall the Royal Society of Chemistry be held responsible for any errors or omissions in this *Accepted Manuscript* or any consequences arising from the use of any information it contains.



Re-interpreted IR spectra: NO with three (a) or five (b) ammonia ligands

39x22mm (300 x 300 DPI)

Ammonia-modified Co(II) sites in zeolites: IR spectroscopy and spin-resolved charge transfer analysis for NO adsorption complexes.†

Kinga Góra-Marek^{1*}, Adam Stępniewski², Mariusz Radoń¹ and Ewa Broclawik^{2*}

¹ *Faculty of Chemistry, Jagiellonian University in Kraków, . Ingardena 3, 30-060 Krakow, Poland*

² *Jerzy Haber Institute of Catalysis PAS, Niezapominajek 8, 30-239 Krakow, Poland*

keywords: NO activation by Co(II) sites, ammonia co-adsorption, IR and DFT modeling, CT analysis

† **Electronic supplementary information (ESI) available:** Optimized geometries and the comparison of calculated charge and spin densities of $[\text{T1Co}(\text{NO})]^+$ and $[\text{T1Co}(\text{H}_2\text{O})_2(\text{NO})]^+$ models; Full list of geometric parameters calculated for studied systems; Comparison of relative energy calculated by various exchange-correlation functionals for singlet (**b_S**) and triplet (**b_T**) of $[\text{T1Co}(\text{NH}_3)_3(\text{NO})]^+$

* *corresponding author: kinga.goramarek@gmail.com*

* *corresponding author: broclawi@chemia.uj.edu.pl*

Abstract

IR spectroscopic studies and quantum chemical modeling (aided by the analysis of charge transfer processes between co-adsorbed ammonia and Co(II)-NO adduct) evidence that donor ammonia molecules, ligated to extraframework Co^{2+} centers in zeolites, vitally affect the strength of the N–O bond. Calculations indicate that versatility of ammine nitrosyl complexes, differing as well in the number of NH_3 ligands as in the geometry and electronic structure of Co-N-O unit (showing variable activation of NO) may co-exist in zeolite frameworks. However, only combined analysis of experimental and calculation results points to the adducts with three or five NH_3 coligands as decisive. The novel finding concerning the interpretation of discussed IR spectra is the assignment of the most down-shifted bands at $1600\text{-}1615\text{ cm}^{-1}$ to the N-O stretch in the singlet $[\text{Co}(\text{NH}_3)_3(\text{NO})]^{2+}$ adduct, in place of tentative ascription to pentaammine adducts. Theory indicates also that the Co(II) center (with manifold of close-lying electronic and spin states) acts as tunable electron donor where the spin state may open or close specific channels transferring electron density from the donor ligands (treated as the part of environment) to the NO molecule.

Introduction

Transition metal exchanged sites in porous materials invariably attract interest of researchers since strict limits imposed on NO emission triggered the development of various catalytic processes to limit pollution released to the atmosphere. Much attention is paid to the selective catalytic reduction (SCR), especially to the SCR with hydrocarbons (including otherwise inert methane).¹⁻³ Cobalt exchanged zeolites were found active in the latter process allowing for effective conversion of NO in oxygen-rich stream and in absence of undesired by-products like CO and N₂O.^{4,5} Favorable structure of the zeolite is frequently reported as very important for catalytic activity of cobalt sites; it is worth noting here that Co-ferrierites exhibit nearly doubled activity in the SCR process compared to Co-ZSM5 at T>500 Deg. C⁶ while the efficiency of Co-ZSM5 catalyst for decomposing NO in the presence of O₂ is one order of magnitude larger relative to Cu-ZSM5⁷. Co(II)-zeolites are also active in other reactions such as SCR of NO with NH₃^{8,9}, ammoxidation¹⁰, oxidation¹¹ or Fischer Tropsch synthesis¹². Therefore, the porous materials containing cobalt sites are still in the center of scientific interest, as well experimental as theoretical¹³⁻¹⁵.

Many factors may influence the overall activity of cobalt sites in zeolites towards NO, in particular the details of the interaction of NO with the adsorption center and the type of the formed bond can decide on both the path of the reaction and the transformation rate of adsorbed molecules. It is well known that unique properties of exchangeable transition metal ions (TMI), partially neutralized by basic oxygen ions from zeolite framework, are responsible for their high ability to activate π -electron molecules. However, neither the kind of an exchangeable transition metal cation or its location, nor the type of zeolitic structure and its chemical composition are the sole factors influencing the activation of the adsorbate. Already the early research by Lunsford *et al.* on nitrosyl complexes of cobalt and copper cations in A, X and Y zeolites has shown that co-ligated ammonia donated electrons upon

binding to the metal sites which activated NO and eventually led to nitric oxide reduction.¹⁶⁻¹⁹ Our former IR spectroscopic studies and quantum-chemical calculations have also indicated that other molecules of the strong electron donor properties ligated to the exchangeable TMI sites may vitally affect the activation of multiple bonds in the adsorbed molecules.^{20,21} It has been evidenced for the co-adsorption of carbon monoxide and organic/inorganic molecules (e.g. alkenes, aldehydes, ammonia, and pyridine) on the Cu⁺ center in zeolite CuZSM-5²⁰, and for ammonia and pyridine co-adsorbed with NO on CoZSM-5²¹. Although the latter studies concerned high-silica zeolites with structural properties different from those characteristic for Y zeolites, very similar effects have been registered. All these findings suggested that significant impact of the electron donor properties of co-adsorbed molecules on the weakening of multiple bonds might offer the opportunity for targeted bond activation.

In this work, IR studies on NO adsorption on ammonia-saturated CoMOR and CoFER zeolites are reported and supplemented by quantum chemical modeling in order to gain detailed insight into the influence of ammonia pre-adsorption on Lewis acidity of cobalt sites and the activation of NO. DFT calculations are done for a consecutive set of models mimicking a Co(II) site hosting as well NO as NH₃ ligands: Co(II)-NO and Co(II)(NH₃)_n-NO (with n = 3 or 5). The choice of the mononitrosyl model for Co(II) site interacting with NO is imposed by the presence of a well-isolated Co(II)-NO species, inferred in our group from the analysis of IR spectra recorded above 600 K for Co-ZSM5 zeolite²¹ while n values are based on experimental protocol. It has also been shown that the pre-adsorption of ammonia may lead to stable mononitrosyls even at room temperature while NH₃ co-adsorption significantly red-shifts the stretching frequency of mono-adsorbed NO.²² On the other hand, NO⁺ and NH₃ alone are also surface species of interest, postulated as conceivable key reaction intermediates of NO-SCR with CH₄ over Co-, (Co,Pt)- and H-mordenite catalysts^{23,24}.

Our former IR experiment²¹ and present results evidence strong red-shift of NO stretching frequency after ammonia pre-adsorption on the sample which implies that co-adsorption of NH₃ enhances backdonation from the cobalt site to NO ligand, in accordance with the work of Lunsford et al.¹⁶⁻¹⁹. Complementary quantum-chemical DFT modeling confirms that upon bonding of additional NH₃ molecules the red-shift of NO stretching frequency shows up; furthermore, the calculations show that the extent of NO activation strongly varies with the type of Co(II)-(NH₃)_n-NO adduct since it depends not only on the number of ammonia ligands, but also on the details of its electronic properties where spin state of the complex may have large effect on the activation ability of cobalt center towards NO. With regard to these findings we have undertaken explicit analysis of charge transfer processes between the co-adsorbed ammonia ligands and the Co(II)-NO core in adducts of various types (with the focus on their relation to donation/backdonation from/to NO antibonding orbitals) to better understand electronic mechanism behind the impact of strong donor co-ligands upon donor properties of the cobalt site.

2. Methods and Models

2.1 Experimental

The parent zeolites NaMOR (Si/Al = 6.5, ZEOLYST, CBV 10 A) and NaFER (Si/Al = 8.8, TOSOH) were ion-exchanged to their ammonium-forms NH₄MOR and NH₄FER. Hereto, the samples were stirred in a 0.5 M NH₄(NO)₃ - solution during 1 h at 353 K (100 mL NH₄(NO)₃ solution/g zeolite). After executing this procedure three times, the zeolites were washed and dried at 385K for 24 h. The ICP results confirmed that all Na⁺ cations have been exchanged. The NH₄MOR and NH₄FER zeolites were undergone the ionic exchange in 0.5M Co(NO₃)₂ solution at 353 K. After exchange procedure, samples were filtered and washed with water until the washing was free from nitrate ions, and dried at 385K for 24 h. The final

samples, designated as 'CoMOR' and 'CoFER', were characterized by an ICP method, revealing $\text{Co/Al} = 0.37$ and $\text{Co/Al} = 0.31$ for CoMOR and CoFER, respectively.

For IR studies a self-sustaining pellet of the sample was prepared, weighted and placed inside the IR cell. Prior to the measurements with the probe molecules, the samples have been degassed at 770 K for 1 h under high vacuum. In all studied cases ammonia (PRAXAIR 99.96%) was adsorbed in controlled amounts. To obtain maximum ligation of NH_3 molecules to Co^{2+} ions an excess of ammonia was adsorbed at 400 K, followed by an evacuation at the same temperature to remove the gaseous and physisorbed ammonia, which has been tracked by the recording of spectra. Subsequently, the FT-IR spectrum was taken at room temperature. The concentration of Lewis sites was calculated using respectively the intensities of the 1620 cm^{-1} band of ammonia coordinatively bonded to Lewis sites (NH_3L) by applying its extinction coefficient. The extinction coefficient of $0.026\text{ cm}^2\ \mu\text{mol}^{-1}$ for the NH_3L band was determined in experiments in which ammonia was adsorbed in dehydroxylated zeolite HY (pre-treated at 1070 K), containing Lewis acid sites as main species.²⁵ Even if the 1620 cm^{-1} band could be due to ammonia interacting with Lewis sites of different nature, i.e. Al- (in dehydroxylated zeolite HY) or Co-Lewis ones (in zeolite under the study), the same value of the extinction coefficient was assumed based on the same value of the $\text{NH}_3\text{-Co}$ and $\text{NH}_3\text{-Al}$ band frequencies. In zeolites under the study only Co^{2+} cations can be considered as Lewis acid sites: neither Na^+ sites nor Al-Lewis sites originated from dehydroxylation were detected. Consequently, the amount of ammonia pre-adsorbed was divided by the number of Co^{2+} cations derived from ICP analysis. For zeolites fully saturated with ammonia the presence of $[\text{Co}(\text{NH}_3)_5]^{2+}$ pentaamminenitrosylcobalt(II) complexes was confirmed. Following the same rule, the $[\text{Co}(\text{NH}_3)_3]^{2+}$ triamminenitrosylcobalt(II) were immobilized in zeolite CoMOR and CoFER. In this case, ammonia was introduced to IR cell in controlled and measured doses up

to the intensity of the 1620 cm^{-1} band of ammonia coordinatively bonded to Co^{2+} sites attained the value corresponding the ratio $3\text{ NH}_3/\text{Co}^{2+}$.

Zeolites hosting both $[\text{Co}(\text{NH}_3)_5]^{2+}$ and $[\text{Co}(\text{NH}_3)_3]^{2+}$ were subjected to the sorption of nitrogen oxide (Linde Gas Polska 99.5%). Sorption of the doses of NO was performed at room temperature up to the appearance of the rotation-vibration bands of gaseous NO. Such procedure assured the reaction of NO molecules with all $[\text{Co}(\text{NH}_3)_5]^{2+}$ and $[\text{Co}(\text{NH}_3)_3]^{2+}$ complexes immobilized in studied zeolites. Consequently, the spectra discussed in this work show the maximum intensities of all NO bands appeared after NO adsorption in zeolites with pre-adsorbed ammonia.

The IR spectra were recorded at room temperature with a Bruker Tensor 27 spectrometer (equipped with an MCT detector) with the spectral resolution 2 cm^{-1} .

2.2 DFT calculations

Geometrical and electronic structure optimizations for studied cluster models were performed by means of Turbomole 5.9²⁶ software within UDFT (unrestricted density functional theory) method with the BP86 exchange–correlation functional and the def2-TZVP basis set provided by the Turbomole package. For discussion of the singlet – triplet splitting we also tested other exchange–correlation functionals (see below).

The performance of the BP86 functional for open-shell adducts between late TM centers and the radical NO ligand has been previously tested by us by comparing selected DFT methods with accurate correlated methods for Fe(II) complexes with NO (in heme and non-heme architectures).^{27,28} It was found that for these $\{\text{Fe-NO}\}^7$ systems, the non-hybrid functionals, like BP86, best reproduced spin density distributions from the multiconfigurational CASSCF approach; importantly, these functionals avoid an excessive spin polarization characteristic of the hybrid functionals. Furthermore, selected iron

complexes, $[\text{Fe}^{\text{II}}(\text{H}_2\text{O})_5(\text{NO})]^{2+}$ and $\text{Fe}^{\text{II}}\text{P}(\text{NH}_3)\text{NO}$, were successfully analyzed in terms of the nature of Fe-NO bond within SR-NOCV (spin-resolved natural orbitals for chemical valence) method, using the DFT/BP86 calculation scheme.²⁸ Moreover, non-hybrid functionals, including BP86, even if imperfect for the energetics, are known to give reliable molecular structures and harmonic frequencies.²⁹ BP86 functional has also been used to evaluate thermodynamics of adsorption of NO on cobalt as a function of the local environments in ferrierite zeolites.³⁰ Recently, a thorough investigation of NO adsorption in Co(II)-exchanged CHA, MOR, and FER zeolites, based on periodic calculations initiated in the group of Hafner,^{15,31-34} also indicated that as well electronic as vibrational properties of Co(II) sites and their mono- and dinitrosyl complexes were predicted with satisfactory accuracy by the non-hybrid functionals.

All these results corroborated our pre-assumption that BP86 functional is a good choice for describing the electronic structure of NO complexes with open-shell cations in a zeolite, including non-innocent $\{\text{Co-NO}\}^8$ systems. Since this work focuses on the impact of electron density deformation upon coordination of additional donor ligands by Co(II) centers onto properties of the NO bond, we base the selection of computational protocol on the performance of BP86 functional with respect to reproducing total electron and spin densities. To this end, some additional tests of the performance of DFT/BP86 method against other functionals, with respect to reproducing spin density and electronic structure from CASSCF calculations (practical with reasonable active space for the minimal conceivable model of the site) have been performed. Detailed studies on the energetic and electronic properties of cobalt complexes with NO by correlated wave function methods are under way in our group and will be published in due time.

Elementary cluster model for the Co(II) site in a zeolite used in this work is based on the simplest conceivable mimic of the framework, e.g. on a single $\text{Al}(\text{OH})_4^-$ tetrahedron

(labeled hereafter as T1). We have already used such model to successfully discriminate between donor properties of Cu(I) and Cu(II) sites in zeolites towards NO.^{35,36} The same model has also been used by us in the CASSCF/CASPT2 studies on mono and dinitrosyls on copper sites in zeolites.³⁷ However, since multiple coordination of Co with the framework should be assumed for majority of zeolitic sites³⁰⁻³⁴, our working model for the Co(II) site is extended here by including two additional water ligands to cobalt to crudely restore fourfold coordination of Co(II) center to basic oxygens. The water ligand as the simplest mimic of a coordinate bond with the basic oxygen has already been used in early modeling studies of cobalt sites.^{30,38} The model proposed here is not neutral, however, we believe that the screening of its effective +1 charge by negative zeolite framework shall merely shift the calculated frequencies, leaving the relative shifts reasonably estimated (see also section 3.3 Vibrational analysis). The minimal cluster applied in our modeling obviously does not allow to discriminate between various zeolite types or cobalt siting; we are fully aware of this shortcoming when relating specific calculation results to experimental data averaged over site speciation.

As compared with bare [(T1)CoNO]⁺ model, addition of two water ligands in the proposed [(T1)Co(H₂O)₂NO]⁺ model somewhat modified Lewis properties of the cobalt center. As expected, the charge on Co cation became slightly more neutralized while the bonding with NO remained essentially unchanged which manifested in negligible shift of NO stretching frequency (by 1.5 cm⁻¹). The improvement due to better mimicking the coordination of the Co²⁺ center manifested in a better localization of spin and electron density on the cobalt in T1Co⁺ fragment. The comparison of geometries, atomic charges and spin densities for [(T1)CoNO]⁺ and [(T1)Co(H₂O)₂NO]⁺ (**a**) is given in ESI. Further studies on the effect of extending cluster models for pertinent cobalt sites (eventually periodic calculations) are under way in our group.

In addition to the primary cluster model $[(T1)Co(H_2O)_2NO]^+$ (**a**) for the adduct of NO with the parent Co(II) site, we consider two model systems for NO adsorption on ammonia-saturated cobalt zeolite: $[(T1)Co(NH_3)_3NO]^+$ (**b**) and $[Co(NH_3)_5NO]^{2+}$ (**c**). We introduce the (**b**) and (**c**) models following the IR experimental results (see section 3.1), suggesting the average numbers of NH_3 ligands coordinated to a single Co(II) site under specified saturation condition as three or five, respectively. Here we assume that the coordination of three strongly bonded ammonia ligands in (**b**) displaces two basic oxygens (simulated in the model by water molecules), while the fivefold ammonia coordination in (**c**) entirely hinders the bonding with the framework. Structure (**c**) as well offers the model for the ammonia-only species proposed on the basis of IR spectrum in fully ammonia-saturated CoMOR zeolites (*vide infra*) as corresponds to the black isomer of pentaamminenitrosylcobalt(II) dichloride^{39,40}.

2.3 SR-NOCV analysis

SR-NOCV (spin-resolved natural orbitals for chemical valence) method^{41,42} is the extended charge decomposition analysis to investigate the electronic relaxation accompanying the formation of a bond between the fragments of the complex system. Complementary alternative schemes based on population analysis of fragment orbitals have also been proposed in the literature,⁴³ however, we continue our study within NOCV methodology where we have already gained expertise in the field of NO bonding to transition metal centers^{28,35,36}. Our previous studies on the interaction of NO with transition metal sites have successfully invoked spin resolution which appeared indispensable to bring novel particulars to the charge transfer analysis, related to the non-innocence of the open-shell NO ligand.

SR-NOCV analysis decomposes the differential density (the difference between electron densities of the final complex and the promolecule) into one-particle contributions, separately for α and β spins. The corresponding promolecule (taken in the geometry of the complex) for each considered system is built of the respective two non-interacting fragments;

herein: the co-adsorbed NH_3 ligands and the Co(II)-NO core, because this work is focused on the influence of ammonia on the bonding within the Co(II)-NO unit. Single point UDFT calculations are performed for the respective fragments in order to compute the differential electron density for each complex. Its diagonalisation provides NOCV orbitals. The pair of the corresponding NOCVs (linked by the modulus of eigenvalues, where the orbital with negative eigenvalue depicts the decrease, and that with positive eigenvalue – the increase of electron density) defines an electron transfer channel between the NH_3 molecules and the Co(II)-NO core. The eigenvalue offers a measure for electron density transferred along a particular charge transfer channel, while the plot visualizes the pathway of electron density transfer (from the region depleted to the region enriched in electron density). Plots are generated with the Gabedit software⁴⁴ from the output of home-made program Natorbs⁴⁵ serving to calculate the NOCV orbitals.

3. Results and Discussion

3.1 IR spectra

The sorption of NO at room temperature in zeolites CoMOR and CoFER have resulted in the formation of dinitrosyl complexes $[\text{Co}(\text{NO})_2]^{2+}$ as the most stable species (Figure 1). Generation of mononitrosyls $[\text{Co}(\text{NO})]^{2+}$ (the species of the lower stability) required thermal decomposition of the dinitrosyls $[\text{Co}(\text{NO})_2]^{2+}$ at 330 °C (Figure 1). Only in such experimental conditions the $[\text{Co}(\text{NO})]^{2+}$ band at ca. 1845 cm^{-1} was detectable. The comparison of the N-O stretching frequency in the mononitrosyl adducts $[\text{Co}(\text{NO})]^{2+}$ (ca. 1850 cm^{-1}) to the gaseous NO (1875 cm^{-1}) evidences a minor activation of NO molecule by Co^{2+} ions bonded to framework oxygen atoms ($\Delta\nu = 25\text{ cm}^{-1}$) (Table 1).

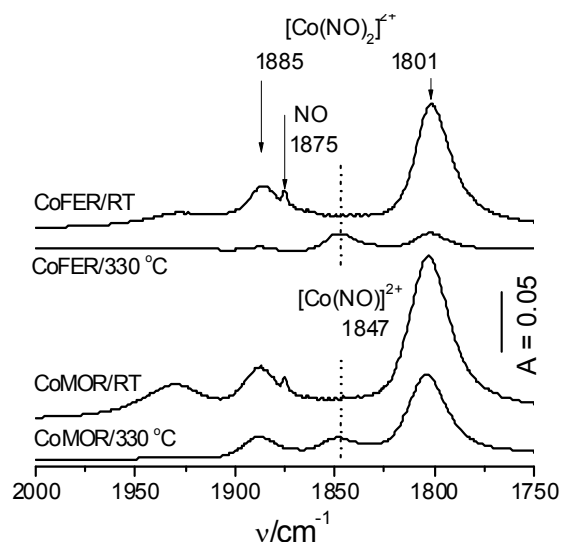


Fig. 1. The spectra of NO adsorbed at room temperature and at 330 °C in zeolites CoFER and CoMOR.

Other series of experiments was designed to evidence the impact of ammonia ligated to the exchangeable Co^{2+} cation on the NO bond. To this end, NO was sorbed in zeolites CoMOR and CoFER with controlled amounts of pre-adsorbed ammonia. Sorption of the measured doses of ammonia in zeolites led to in the appearance of the 1620 cm^{-1} band of NH_3 bonded coordinatively to cationic sites, $\text{H}_3\text{N-Co}^{2+}$. After adsorption of consecutive ammonia doses, the intensity of the 1620 cm^{-1} band (due to H-N-H bending) was measured and used to evaluate the average number of ammonia molecules interacting with one Co^{2+} cation. The value of the applied extinction coefficient was typical of the Al-originated Lewis sites ($0.026\text{ cm}^2\mu\text{mol}^{-1}$)²¹. Even if the 1620 cm^{-1} band could be due to ammonia interacting with Lewis sites of different nature, i.e. Al- or Co-Lewis ones, the same value of the extinction coefficient was assumed based on the same value of the $\text{NH}_3\text{-Co}$ and $\text{NH}_3\text{-Al}$ band frequencies. In this way, the average numbers of NH_3 molecules interacting with one Co^{2+} cation in distinct samples have been evaluated as 3 NH_3/Co and 5 NH_3/Co , respectively (depending on the zeolite and sample type).

The sorption of NO in CoMOR and CoFER zeolites treated with the dose of ammonia corresponding to three NH₃ per Co²⁺ site (*vide supra*) has evidenced a significant red shift of the NO band attributed to the formation of the [Co(NH₃)₃(NO)]²⁺ complexes. Analysis of the differential spectrum of NO sorbed in CoMOR zeolite accommodating [Co(NH₃)₃]²⁺ adducts has revealed the development of two mononitrosyl [Co(NH₃)₃(NO)]²⁺ bands (1765 and 1745 cm⁻¹) pointing to the heterogeneity of Co(II) siting⁴⁶ with variable neutralization of the positive charge of Co²⁺ cations in the [Co(NH₃)₃(NO)]²⁺ adducts (Figure 2, spectrum a). For zeolite CoFER only one band at 1730 cm⁻¹, assigned to [Co(NH₃)₃(NO)]²⁺ complex (Figure 2, spectrum b) has been identified. In general, a vital feature of NO in [Co(NH₃)₃(NO)]²⁺ adducts is the significant downshift of N-O vibration with respect to the frequency of NO in the gas phase ($\Delta\nu = 130\text{-}110\text{ cm}^{-1}$). It indicates that the NO bond in the [Co(NH₃)₃(NO)]²⁺ complexes is substantially weakened. The presence of the 1750 cm⁻¹ band has additionally been reported for zeolite CoZSM-5²¹ where it was tentatively assigned to the mononitrosyls with four NH₃ ligands. The weakening of N-O bond, evidenced by the significant red shift, may be related to the back donation of electrons from basic ammonia molecules *via* Co²⁺ to antibonding π^* orbitals on NO molecule. Assuming the same number of NH₃ molecules per Co site (i.e., 3), i.e., the existence of [Co(NH₃)₃(NO)]²⁺ complexes in both MOR and FER zeolites, different π^* -backdonation ability of Co²⁺ cations in these zeolites can be assigned to variable speciation of cobalt sites in these zeolites, including Si/Al ratio, site location or geometric features of the framework. All these factors could lead to variable extent of the neutralization of Co²⁺ cations by the negative framework; theoretical modeling at molecular level has been undertaken in the hope to partially unravel determinants influencing the status of the cobalt center.

Moreover, for both MOR and FER zeolites the presence of significantly red shifted band at 1615 cm⁻¹ was also detected. In the light of quantum chemical calculations (presented

in sections 3.2) as well the band at ca. 1615-1610 cm^{-1} as that at 1765-1730 cm^{-1} can be assigned to the $[\text{Co}(\text{NH}_3)_3(\text{NO})]^{2+}$ species in alternated electronic (in particular spin) states.

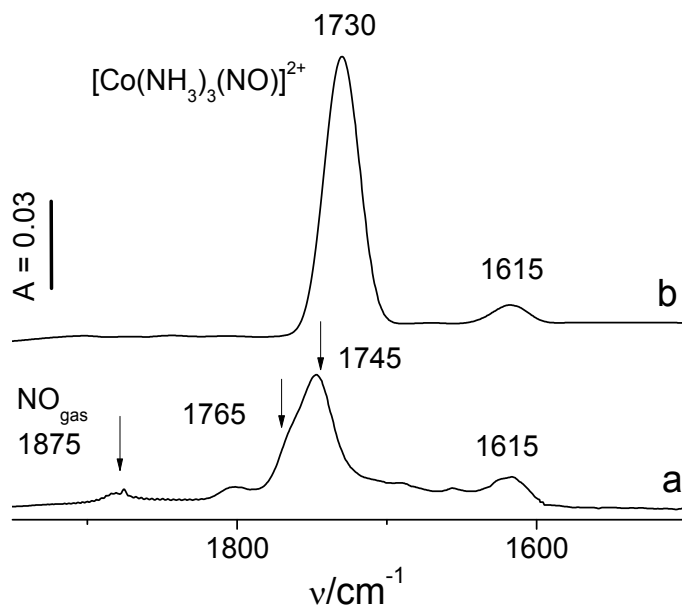


Fig. 2. The spectra of NO adsorbed in zeolites CoMOR (a) and CoFER (b) hosting the $[\text{Co}(\text{NH}_3)_3]^{2+}$ complexes

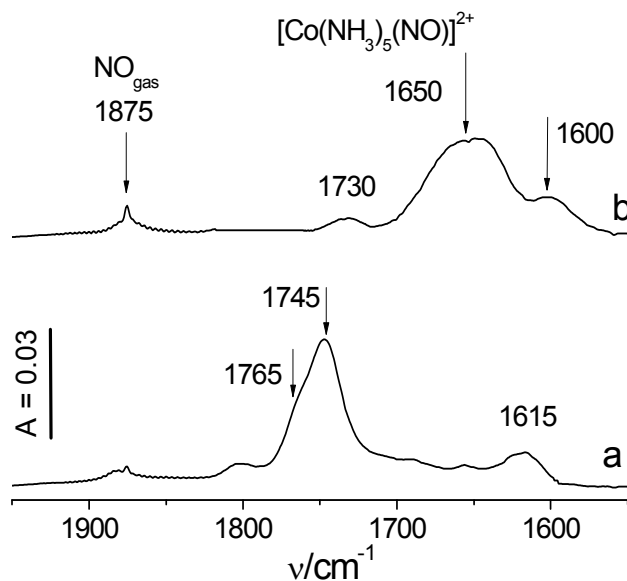


Fig. 3. The spectra of NO adsorbed in zeolite CoMOR accommodating $[\text{Co}(\text{NH}_3)_3]^{2+}$ (a) and $[\text{Co}(\text{NH}_3)_5]^{2+}$ complexes (b).

The sorption of NO was also performed in CoMOR zeolite pretreated with the highest doses of ammonia and presumably hosting the $[\text{Co}(\text{NH}_3)_5]^{2+}$ pentaammine complexes, i.e. holding Co^{2+} cations nearly saturated by ammonia molecules. The sorption of NO has resulted in appearance of the complex band centered at 1650 cm^{-1} , the origin of which are immobilized pentaamminenitrosylcobalt(II) complexes (Figure 3, spectrum b). A weak band around 1600 cm^{-1} is also noticeable for these samples. The $[\text{Co}(\text{NH}_3)_5(\text{NO})]^{2+}$ complexes are widely known in the cobalt coordination chemistry and usually regarded as NO^- complexes of Co(III). In such $[\text{Co}^{(\text{III})}(\text{NH}_3)_5(\text{NO}^-)]^{2+}$ complexes complete electron transfer from Co^{2+} to NO was postulated: the Co^{3+} oxidation state is stabilized by NH_3 and other electrodonor ammonia ligands, as well as by CN^- in $[\text{Co}(\text{CN})_5(\text{NO})]^{3-}$ complexes. The very low frequency for the NO stretching vibration when NO gains electron density has been commonly accepted;^{43,44} for these compounds the +3 oxidation state has been attributed to the cobalt and the NO stretching frequency was assigned to the bands between 1550 and 1650 cm^{-1} .^{47,48} In consequence, very strong impact of the electron donor properties of co-adsorbed molecules on the weakening of multiple bonds should provide the opportunity for targeted N-O bond activation.

It should be additionally noted that the $[\text{Co}(\text{NH}_3)_5(\text{NO})]^{2+}$ complexes have been formed in zeolite CoFER only in negligible quantities. While mordenite is considered as a 12-ring structure, ferrierite is only a 10-ring zeolite, thus the framework topology restrictions may be responsible for the absence of bulky $[\text{Co}(\text{NH}_3)_5(\text{NO})]^{2+}$ complexes.

3.2 Structural and electronic properties of cluster models

Optimized structures of the studied models (a) – (c) are shown in Fig. 4. We examine in detail the triplet state for (a) and the singlet for (c). For the parent Co(II) site we follow suggestions inferred from former works³⁰⁻³⁴ where a spin of $S = 1$ in Co(II) sites and their adducts with nitrosyl, arising from localized spins with opposite orientations on the high-spin

Co cation and the NO ligand was proposed. Nevertheless, the singlet state for **(a)** was also tested but as well the geometry, electronic and vibrational properties as the energetic separation from the ground-state triplet indicates that both structures are nearly equivalent. The comparison of the Co-O bond lengths with periodic models studied by Göttl et al.³¹⁻³⁴ shows that the cluster model $[(T1)Co(H_2O)_2NO]^+$ **(a)** reasonably mimics the bonding with four framework oxygens (compare the distances of 2.19, 2.19, 1.97 and 1.97 Å in cluster model to the distances in the range of 1.85 to 2.36 Å obtained by DFT/PBE in periodic models, depending on the cobalt siting). Next, ammonia ligands were consecutively added, constituting ammonia-saturated **(b)** and **(c)** adducts. Furthermore, we assume that five strongly interacting ammonia ligands suppress the spin on cobalt cation to the low-spin state in **(c)**; additional arguments in favor of the singlet come from the comparison of geometric parameters calculated for the singlet complex **(c)** with experimental crystal structure of pentaamminenitrosyl cobalt(II) dichloride (*vide infra*). In variance, for the intermediate **(b)** model with three coordinated NH_3 ligands as well the singlet (S) as triplet (T) spin states are scrutinized for further analysis since these two states show very distinct geometric and vibrational properties while being very close in energy. Full listing of structural parameters for the triplet **(a)**, the singlet **(c)**, and singlet and triplet states **(b_S)** and **(b_T)**, along with the comparison of singlet-triplet splitting for **(b)** calculated by various exchange-correlation functionals are given in ESI. Table 2 lists selected geometric parameters relevant for NO activation (the Co-N-O angle, Co-N and N-O distances) for models **(a)**, **(b_S)**, **(b_T)** and **(c)**.

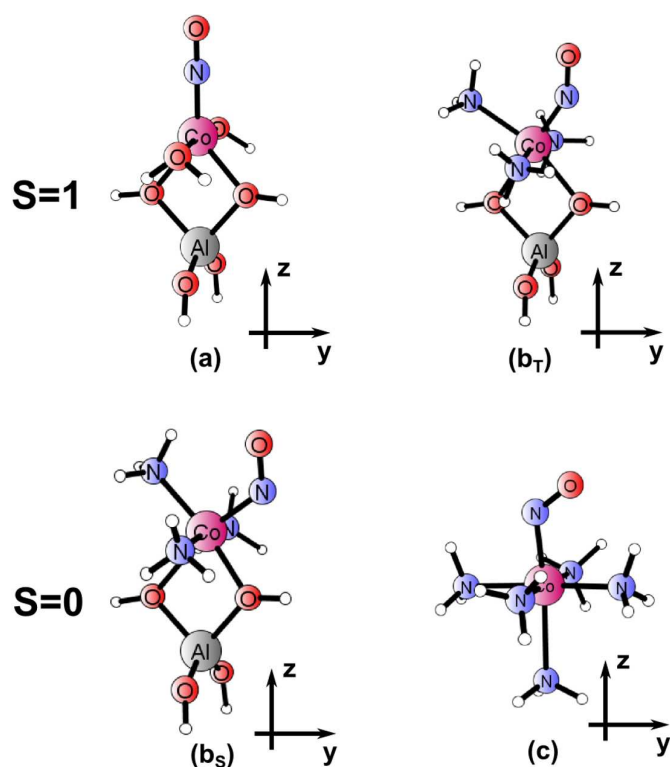


Fig. 4. DFT-optimized structures of triplet models for NO adducts with Co(II) sites: with no ammonia (parent model **(a)**, GS), three ammonia co-ligands (**(b_T)**) and of singlet models for three (**(b_S)**) or five (pentaamminenitrosylcobalt(II) **(c)**, GS) ammonia co-ligands

Model **(a)** (Figure 4**(a)**) has a linear Co-N-O motif and is used as a reference to analyze the NO bonding by a non-modified cobalt site. For the complex with three ammonia ligands, the singlet adduct **(b_S)** has a strongly bent Co-NO unit (122°), while the triplet structure **(b_T)** shows a moderate bend of the Co-N-O motif (148°). In the case of the singlet **(c)** adduct the coordination of five ammonia ligands (hindering the bonding of cobalt cation to the zeolite fragment) makes the Co-N-O unit strongly bent. The two spin states in the **(b_S)** and **(b_T)** complexes are nearly degenerate in energy. The BP86 functional points to the singlet lying only 5.2 kcal/mol below the triplet but the energy difference (and even its sign) are strongly functional-dependent (the comparison with other GGA and hybrid functionals is given in ESI). Hence we conclude here that both spin states may coexist in reality.

Furthermore, in order to test reliability of the assumption that the coordination with strong ammonia donors may compete with additional Co-O bonds to the framework, we have calculated the energy gain while going from complex (a) to complex (b_T). The exchange of two water ligands by two NH₃ ligands (an intermediate stage to the formation of (b), with very similar structure to that of [(T1)Co(H₂O)₂NO]⁺ one) is exothermic by as much as 22.5 kcal/mol. Addition of the next ammonia ligand to give (b_T) still lowers the energy (by another 22.2 kcal/mol). In view of the well-known strong dependence of the calculated adsorption energies on the choice of exchange-correlation functional we have additionally inspected this aspect. Tests with B3LYP functional evidenced that in the cobalt case the dependence was not dramatic: the exchange of water by ammonia ligands yielded energy gain by 16.6 kcal/mol while the addition of the third ammonia ligand yielded the energy gain by 21.8 kcal/mol.

Detailed analysis of the spin density for model complexes brings an interesting insight into their electronic structure. Spin density distribution for complex (a) (shown in Fig. 5a) confirms that the triplet spin state stems from an antiferromagnetic coupling of the quadruplet Co²⁺ (with the occupations $d_{xy}^2 d_{yz}^2 d_{xz}^{\uparrow} d_{z^2-x^2}^{\uparrow} d_{y^2}^{\uparrow}$) with the unpaired electron on the NO ligand (π_x^{\downarrow}). This interpretation agrees with that discussed in ref. 33; however, it must be stressed here that due to cylindrical symmetry of the Co-N-O unit, the actual electronic structure of the complex should involve the second equivalent configuration, namely $d_{xy}^2 d_{yz}^{\uparrow} d_{xz}^2 d_{z^2-x^2}^{\uparrow} d_{y^2}^{\uparrow}$, antiferromagnetically coupled to π_y^{\downarrow} on NO. Therefore, fully correct description of this complex would call for multiconfiguration wavefunction methodology and such a study is under way in our group.

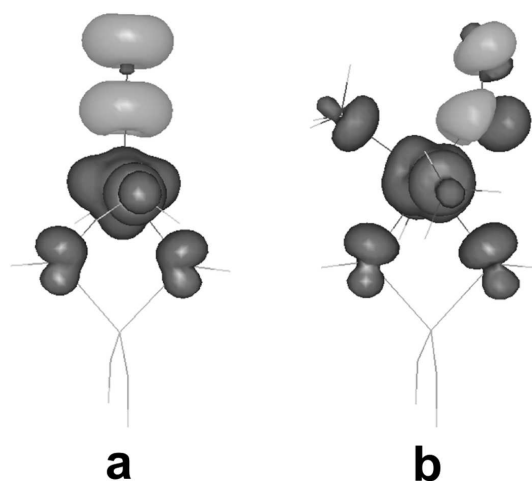


Fig. 5. Spin densities for triplet complexes: $[(T1)Co(H_2O)_2NO]^+$ (a) and $[(T1)Co(NH_3)_3NO]^+$ (b); dark grey – majority spin, light grey – minority spin, contour value of 0.003.

For the triplet complex comprising three ammonia ligands (**b_T**), the spin distribution (shown in Fig. 5b) also suggests an electronic configuration, inferred from the quadruplet cobalt cation (with the occupations $d_{xz}^2 d_{\perp}^2 d_{\parallel}^{\uparrow} d_{x_2 y_2}^{\uparrow}$) antiferromagnetically coupled to $\pi_{\parallel}^{*\downarrow}$ on NO. Due to rotation of the axis pointing along the Co-N bond, the notation d_{\parallel} and d_{\perp} (with respect to the Co-N-O plane) is used here. The major difference between the two triplet states is related to the bent geometry of the Co-N-O unit in the latter, which enables a weak σ coupling between the d_{\parallel}^{\uparrow} and $\pi_{\parallel}^{*\downarrow}$ orbitals, and makes the empty π_{\perp}^* on NO ready for backdonation from doubly occupied cobalt d_{\perp} orbital. The two singlets, (**b_S**) and (**c**) have closed shell electronic structure attributable to the configuration $d_{xz}^2 d_{\perp}^2 d_{yz}^2 \sigma_{Co-NO}^2 d_{x_2}^0 \pi_{\perp}^{*0}$. Here again, the strongly bent NO geometry is favorable for making a strong σ bond as well as for significant backdonation from the doubly occupied d_{\perp} to the empty π_{\perp}^* on NO. These electronic parameters may be related to the activation of NO bond evidenced by IR red shift of its stretching frequency (as discussed in the following paragraphs).

Only in the case of complex (**c**) structural parameters may be compared to the measured crystal structure of $[Co(NH_3)_5NO]^{2+}$ cation in pentaamminenitrosylcobalt(II)

dichloride.³⁹ The comparison of calculated and experimental structural data (see Table 2) indicates good agreement with the crystal structure which may be taken as an indirect experimental support in favor of the singlet ground state for the black isomer of this complex.

3.3 Vibrational analysis

Table 3 compares the values of NO stretching frequency calculated for NO interacting with models mimicking various Co(II) sites (in non-modified or ammonia-saturated zeolites) with the measured ones (averaged over zeolite types and site speciation for the bands). The assignment of the models to IR bands registered for $[\text{Co}(\text{NH}_3)_3(\text{NO})]^{2+}$ and $[\text{Co}(\text{NH}_3)_5(\text{NO})]^{2+}$ adducts is based on scrutinized re-inspection of experimental spectra in the context of the closest correspondence between the calculated and measured frequencies and is given in the second column (cf. section 3.1). Our detailed analysis suggests that the most red-shifted NO band does not correspond to the highest number of ammonia ligands, but to the intermediate saturation with three donor ligands per site, albeit with the spin on the cobalt cation reduced from the quadruplet (in the parent Co(II) site) to the doublet. The singlet state for the complex comes from the coupling of Co^{2+} ($S=1/2$) with the unpaired electron on NO. The same resultant singlet spin state emerges for pentaamminenitrosyl Co(II) complex, but both calculated and measured red-shifts are lower than for the singlet adduct with three NH_3 ligands. Table 3 lists also the calculated total charge and spin densities on the adsorbed NO. It is clear that co-adsorption of electron-donating ammonia ligands substantially red-shifts stretching frequency of NO which is evidenced as well by the experiment as by the calculation; however, only DFT modeling revealed that the extent of NO activation critically depends also on particulars of the electronic structure (e.g. spin state) of the adduct. In view of the limitations put on the accuracy of calculation results by the simplified, positively charged cluster model and harmonic approximation, the overall agreement of theoretical results with the trends observed in experiment is acceptable. Larger error in the case of model

(c) may be ascribed to complete negligence of charge screening due to the embedding in electron-rich zeolitic environment; the source of error with respect to the actual amminitrosylcobalt(II) dichloride may be rooted in other factors, e.g. negligence of nearest neighbors in the crystal lattice. For the parent complex (a) the calculations give blue-shift instead of a minute red-shift in the experiment; however, this effect is already well-known from previous studies where these shifts in the range of $+57 \div +86 \text{ cm}^{-1}$ were found with equivalent GGA PBE functional for periodic models of real zeolites^{15, 33,34}.

The calculated red-shift of the NO stretch due to ammonia co-ligation is generally underestimated (by 24 to 41 cm^{-1}) with respect to the experiment but the trend in shifts attributed to additional ammonia co-ligands is reasonably reproduced. The most important observation is that theory predicts versatility of possible forms for the $[\text{Co}(\text{NH}_3)_n(\text{NO})]^{2+}$ adducts, diverse not only by the number of ammonia molecules, but also by the spin state and by the geometry of Co-N-O unit. The energy separation between spin states is small and strongly functional-dependent (the singlet is generally favored for ammonia-ligated adducts by the DFT/BP86 calculation), thus it may be rather suggested that various forms may coexist in real zeolites and under ambient conditions. In consequence, only the ranges of experimental frequency red-shifts may be used as the reference to calculation since the emergence of selected distinct forms may depend on the zeolite type and on experimental conditions (not accounted for by the present small models). Earlier DFT calculations for periodic models of NO adsorption on cobalt sites in chabazite, mordenite, and ferrierite zeolites^{15,30,33,34} also pointed to the existence of diversity of NO adducts in the zeolite framework, showing different geometries and frequencies.

Nevertheless, the novel finding concerning the interpretation of the discussed IR spectra (stemming from DFT modeling) is the proposal to assign the most down-shifted bands

at 1600-1615 cm^{-1} rather to the singlet state of $[\text{Co}(\text{NH}_3)_3(\text{NO})]^{2+}$ adduct than to a feature belonging to the spectrum of pentaammine adducts (released to the cavity, the latter practicable in selected zeolite types with sufficiently large cavities). This could not be foreseen without scrutinized calculations.

In addition to the calculated stretching frequencies, theoretical modeling gives also specific information not accessible from the experiment, such as geometrical parameters (Table 2) and electron or spin populations on NO ligand (Table 3), presumably evidencing donation/backdonation processes. Unfortunately, neither of these descriptors satisfactorily correlates with the absolute red-shift of NO stretching frequency (either measured nor calculated). Even if some crude relation of the red shift to the bending of NO unit and diminishing of positive charge on NO might be noticed, neither the charge nor spin density on NO fully rationalizes the postulated occurrence of strong backdonation.

3.4 Interpretation of SR-NOCV analysis

In our former papers we have already postulated that the analysis of independent electron density flow channels (depicting virtual charge transfer processes) was able to properly identify the source of ligand activation.^{28,35,36,49-54} Therefore, in order to quantify the influence of additional donor ligands to the cobalt center on its donation/backdonation ability, for the complexes with three ammonia ligands (in singlet and triplet states, \mathbf{b}_S and \mathbf{b}_T) and with five ammonia ligands (\mathbf{c}) we have scrutinized the analysis of the differential density (calculated for the promolecule built from ammonia ligands shell as the one fragment and the reminder of the Co(II)-NO core as the other fragment). Since the spin on the closed-shell fragment corresponding to the ammonia ligands is always singlet, the spin on the other fragment is unambiguously set to the singlet for (\mathbf{b}_S) and (\mathbf{c}), and to the triplet for (\mathbf{b}_T). The dominant orbital and spin resolved charge transfer channels (defined by the NOCVs with an

eigenvalue modulus larger than the threshold of 0.1), serve here to quantify the transfer of electron density from the NH_3 lone pairs to the Co(II) center and to the NO ligand.

We recall that the three models, (**b_S**), (**b_T**) and (**c**), subjected to the analysis, have been found in section 3.3 to present interestingly distinct vibrational properties: the triplet $\text{Co(II)(NH}_3)_3(\text{NO})$ adduct (**b_T**) reproduces the red shift of NO stretching frequency corresponding to the IR band routinely attributed by experiment to three NH_3 molecules ligated to Co(II) site, whereas its singlet counterpart (**b_S**) offers strikingly distinct activation ability and, unexpectedly, reproduces the most red-shifted IR band, formerly overlooked in experimental studies. Model (**c**) reproduces the properties of the pentaammine cobalt adduct invoked in experimental interpretation of IR spectrum for fully ammonia-saturated cobalt zeolites.

The resultant NOCV independent charge flow channels, plotted according to the convention ascribing red contours to the depletion and blue contours to the gain of electron density, are shown in Figures 6 and 7 for the models in the triplet or the singlet state, respectively. We can interpret each channel as corresponding to the electron flow upon the bond formation from the red area to the blue region. The corresponding eigenvalue is given together with the contour plot for each channel and serves for estimating the number of electrons redistributed along this channel (i.e., to quantify its efficiency in the total charge transfer between the fragments). The assumed partition scheme allows direct visualizing the influence of ammonia co-adsorption on the electron density redistribution within the Co-N-O core by inspecting resulting charge flow channels between NH_3 ligands and the remainder of a particular model. Figures 6 and 7 show solely the selected channels, characterizing the influence of ammonia co-ligation on the NO bond.

Fig. 6 shows spin-resolved channels for the triplet (\mathbf{b}_T) model. Only one channel (in spin majority manifold, with the eigenvalue of 0.46), describes the effective flow of α electron density from three ammonia lone pairs to NO. The corresponding channel for β spin manifold depicts merely density flow from ammonia lone pairs to the cobalt center without participation of NO ligand, and thus it is assumed here not directly related to NO activation. In variance, for the two singlet structures (\mathbf{b}_S) and (\mathbf{c}), Fig. 7) there are two cumulative ($\alpha+\beta$) channels with large eigenvalues .

Since the eigenvalues quantify the channel efficiency (i.e. the amount of transferred electron density) these channels may be directly taken as the signature of the increase in backdonation ability of the site to the antibonding π^* orbital on NO and thus its activation propensity towards NO. In summary, after ligation of ammonia molecules to the cobalt center significant transfer of electron density from donor ligands via the Co(II) core to the antibonding orbital on NO ligand shows up, which nicely corroborates the experimental interpretation of relevant IR spectra. However, its quantitative ratio and thus the expected effect on the NO bond activation depends not only on the number of donor ligands, but also on the spin state of the system. This suggests that the particulars of the electronic structure of the Co(II) center may play a vital role in opening or closing specific electron transfer channels between the site and NO ligand.

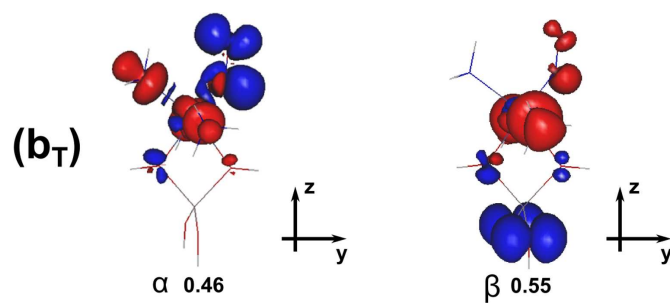


Fig.6. Dominant spin-resolved (α or β) electron transfer channels for the triplet (\mathbf{b}_T) model with corresponding eigenvalues (blue: accumulation, red: electron density depletion; contour value 0.001)

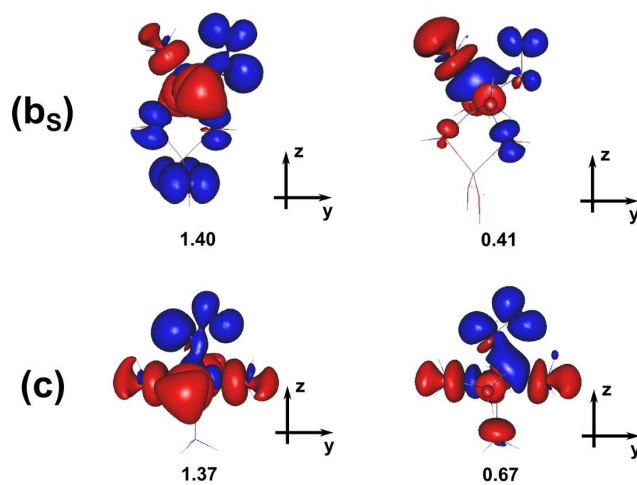


Fig.7. Dominant cumulative ($\alpha+\beta$) electron transfer channels for the singlet models (\mathbf{b}_S) and (\mathbf{c}) with corresponding eigenvalues (blue: accumulation, red: electron density depletion; contour value 0.001).

4. Summary and conclusions

Table 4 summarizes experimental and calculated *relative* shifts of NO stretching frequency ($\Delta\Delta v_{\text{NO}}$) in the studied systems hosting one or five ammonia ligands, with respect to NO adsorbed on a parent cationic Co(II) site in a zeolite (modeled as $[(\text{T1})\text{Co}(\text{H}_2\text{O})_2(\text{NO})]^+$). Relative shifts $\Delta\Delta v_{\text{NO}}$ calculated for the singlet or triplet ((\mathbf{b}_S) or (\mathbf{b}_T)) and the singlet ((\mathbf{c})) states are listed along with the descriptor for electron transfer from the ammonia ligands to the NO (estimated from the corresponding NOCV eigenvalues). The correspondence between the relative shift of NO stretching frequency due to ammonia co-adsorption and the amount of electron density transferred from the lone pairs on NH_3 ligands to π^* antibonding orbital on NO is very good. This is especially important observation if we recall the lack of strict correlation between Δv_{NO} and other electronic factors like the charge or spin on NO (frequently used for estimating the direction and magnitude of charge transfer).

Obviously, we do not claim that the calculated estimates of $\Delta\rho^{\text{NOCV}}_{\text{NH}_3\rightarrow\text{NO}}$ offer fully quantitative measure of charge transfer between the two types of ligands because we are aware that neither the models for Co(II) sites fully mimic properties of zeolite environment nor is the model (\mathbf{c}) a perfect mimic of pentaammine-coordinated Co(II)-NO, weakly bound in a zeolite framework. In addition, semi-quantitative assignment of electron-depleted or electron-enriched contours to the fragments depends on the type of the formed bond; prospective impact of the embedding (e.g. electrostatic field created by the framework) is also entirely neglected. Moreover, it must be stressed here that reliable analysis of the electron density transfer between pre-defined fragments requires as well proper selection of the non-interacting fragments as in-depth understanding of the electronic structure (e.g. spin states) of the complex containing non-innocent ligands, which not always is a routine and unarguable venture²⁸. Significant improvement in agreement when comparing *relative* experimental to

relative calculated red-shifts (taken with respect to the red-shift obtained for the Co(II) site in a pure zeolite) suggests that the influence of the environment of the cobalt cation in the adducts (modeled as either $[T1Co(H_2O)_2(NO)]^+$ or $[T1Co(NH_3)_n(NO)]^+$) greatly cancels out (*all* calculated relative red shifts are underestimated by ca. 40-50 cm^{-1}). The correspondence between the *relative* red-shift of NO stretching frequency (ascribed to ligation of donor ligands) and the increase of the population on the π^* antibonding orbital of NO due to additional electron density transfer from lone pairs on ammonia ligands is well featured by the designed analysis of charge transfer processes.

In general, we have shown that electron-donating ligands strongly influence the status of the site; however, the degree of their impact on the NO co-adsorbed on the same transition metal center depends dramatically as well on the spin as on the adduct type. Obviously, the type of the metal itself is also of major importance (compare cobalt to copper sites^{35,36}) but definitely, the featured electronic structure of the complex determines the final effect for cobalt. In the case of Co(II) sites with co-adsorbed ammonia, not only the number of donor co-ligands but also the spin state of the adduct appeared to be crucial for the performance of the Co(II) core (opening or closing direct channel for electron transfer). Thus the cobalt center may act as tunable electron transmitter between the co-adsorbed ligands, here electron-donating NH_3 and the target NO molecule.

Finally, the comprehensive interpretation of the region of IR spectrum attributed to ammonia-modified Co^{2+} sites in zeolites, proposed on the basis of joint IR experiment and DFT modeling, may be summarized as follows. The region corresponding to the NO stretch at 1765-1730 cm^{-1} may be unequivocally assigned to the triplet $Co(II)(NH_3)_3(NO)$ adducts. The formation of this adduct is supported by DFT calculated binding energies, indicating that substitution of two basic oxygens by NH_3 donor ligands is favored thermodynamically; the

binding energy for the third ligand is also substantial. The strongly red-shifted bands centered at 1650 cm^{-1} registered for fully ammonia-saturated zeolites are firmly attributed to $\text{Co(II)-(NH}_3)_5\text{-NO}$ adducts. Furthermore, DFT modeling offers novel interpretation for the most red-shifted band at $1600\text{-}1615\text{ cm}^{-1}$, as attributable to the singlet state of the $\text{Co(II)-(NH}_3)_3\text{-NO}$ adduct. This band shows up after NO sorption on cobalt sites after as well medium as full saturation with ammonia. This might be explained by conceivable coexistence of both spin states of the $\text{Co(II)-(NH}_3)_3\text{-NO}$ adducts after NO sorption for the intermediate saturation with ammonia and by the coexistence of all $\text{Co(II)-(NH}_3)_n\text{-NO}$ forms after NO sorption on fully ammonia-saturated zeolite. This versatility of Co(II) sites with varying activation abilities indicates that the Co(II) center acts as tunable electron donor where the spin state may open or close specific channels transferring electron density from the environment (treated as an electron reservoir) to the NO molecule.

The case study for NO adsorption on ammonia-saturated zeolites (by IR-assisted quantum chemical modeling) partly explains why the interpretation of the activity of cobalt sites in zeolites towards NO poses significant challenges and piles-up unresolved queries. We have shown that versatility of adducts, differing in geometry, electronic structure (modeling) and by the activation of NO (evidenced both by modeling and IR spectroscopy), may co-exist in zeolite frameworks. Their balance and thus the apparent activity towards NO depends on fine structural features of a particular zeolite and on experimental conditions. These aspects remain to be investigated in future studies.

Acknowledgments

The IR study was financed by Grant No. 2013/09/B/ST5/00066 from the National Science Centre, Poland. DFT modeling was funded by Grants No. 2011/01/B/ST4/02620 from the National Science Centre, Poland and by Marian Smoluchowski Krakow Research Consortium (Leading National Research Centre, KNOW).

Table 1. IR experimental N-O stretching frequencies of gaseous NO and NO in the $[\text{Co}(\text{NO})]^{2+}$ and $[\text{Co}(\text{NH}_3)_n(\text{NO})]^{2+}$ mononitrosyl complexes (re-interpreted weak features given in italics).

Zeolite	Si/Al	NO frequencies/cm ⁻¹			
		NO _{gaseous}	Co(II)-NO	[Co(II)(NH ₃) ₃]-NO	[Co(II)(NH ₃) ₅]-NO
CoFER	8.8	1875	1847	1730	<i>1615</i>
CoMOR	6.5		1852	1765, 1745	<i>1600, 1650</i>

Table 2. Selected DFT-optimized parameters relevant for NO activation (Co-N-O angle, Co-N and N-O distances) for complexes of NO with studied models of Co(II) sites: parent $[\text{TlCo}(\text{H}_2\text{O})_2]^+$ cluster and the adducts with ammonia ligands, (*available experimental values for pentaamminenitrosylcobalt(II) complex from ref. 39 in italics*).

	$[\text{TlCo}(\text{H}_2\text{O})_2(\text{NO})]^+$	$[\text{TlCo}(\text{NH}_3)_3(\text{NO})]^+$		$[\text{Co}(\text{NH}_3)_5(\text{NO})]^{2+}$
Model	(a)	(b_S)	(b_T)	(c)
$\alpha_{\text{Co-N-O}}/\text{deg}$	180	122	148	122.5 (<i>119</i>)
$d_{\text{Co-NO}}/\text{\AA}$	1.69	1.79	1.70	1.84 (<i>1.87</i>)
$d_{\text{N-O}}/\text{\AA}$	1.14	1.19	1.16	1.17 (<i>1.15</i>)

Table 3. The comparison of calculated (for all types of models) and experimental (averaged over all zeolite types) shifts of NO frequency with respect to the molecule in the gas phase; calculated charge and spin densities on NO.

Model	Interpretation	$\Delta\nu_{\text{NO}}^{\text{exp}}/\text{cm}^{-1}$ ^{a)}	$\Delta\nu_{\text{NO}}^{\text{calc}}/\text{cm}^{-1}$	Q^{NO} ^{b)}	$\rho_{\text{S}}^{\text{NO}}$ ^{b)}
(a)	Co(II)-NO	$(-7)^{\text{av}}$	+74	+0.22	0.43
(b_T)	Co(II)(NH ₃) ₃ -NO S=1	$(-109)^{\text{av}}$	-80	+0.10	0.13
(b_S)	Co(II)(NH ₃) ₃ -NO S=0	$(-250)^{\text{av}}$	-226	-0.03	0
(c)	Co(II)(NH ₃) ₅ -NO	$(-207)^{\text{av}}$ $(-247)^{\text{d}}$	-166^{c}	+0.07	0

^{a)} with respect to free NO (calc. $\nu_{\text{NO}} = 1883.56 \text{ cm}^{-1}$); ^{b)} from Mulliken population analysis; ^{c)} model completely neglecting framework embedding; ^{d)} pentaamminenitrosylcobalt(II) dichloride, after ref. 40

Table 4. Experimental and calculated relative shifts of NO stretching frequency ascribed to three or five ammonia co-ligands ($\Delta\Delta\nu_{\text{NO}}$ relative to a parent Co(II)-NO species); estimated numerical descriptors for electron transfer from ammonia ligands to NO ($\Delta\rho^{\text{NOCV}}_{\text{NH}_3\rightarrow\text{NO}}$).

Property	Three NH ₃ ligands		Five NH ₃ ligands
	Triplet	Singlet	Singlet
$\Delta\Delta\nu_{\text{NO}}^{\text{exp}}/\text{cm}^{-1}$	(-102) ^{av}	(-243) ^{av}	(-200) ^{av}
$\Delta\Delta\nu_{\text{NO}}^{\text{calc}}/\text{cm}^{-1}$	-154	-290	-240
$\Delta\rho^{\text{NOCV}}_{\text{NH}_3\rightarrow\text{NO}}$	0.5	< 1.8	< 2.0

References

- ¹ Y. Traa, B. Burger, J. Weitkamp, *Micropor. Mesopor. Mater.*, 1999, 30, 3.
- ² M. Iwamoto, *Stud. Surf. Sci. Catal.*, 2000, 130A, 23.
- ³ A. E. Palomares, C. Franch, A. Corma, *Catal. Today*, 2011, 176, 239.
- ⁴ D. Pietrogiacomini, M.C. Campa, V. Indovina, *Catal. Today*, 2010, 155, 192.
- ⁵ M.C. Campa, S. De Rossi, G. Ferraris, V. Indovina, *Appl. Catal. B: Environ.*, 1996, 8, 315.
- ⁶ Y. Li, J. N. Armor, *Appl. Catal. B: Environ.*, 1993, 3, 1.
- ⁷ Y. Chang, J. G. McCarty, *J. Catal.*, 1998, 178, 408.
- ⁸ T. Montanari, O. Marie, M. Daturi, G. Busca, *Catal. Today*, 2005, 110, 339.
- ⁹ T. Grzybek, J. Klinik, M. Motak, H. Papp, *Catal. Today*, 2008, 137, 235.
- ¹⁰ Y. Li, J.N. Armor, *J. Catal.*, 1998, 176, 495.
- ¹¹ J.H. Thomas, *Adv. Chem. Ser.*, 1995, 246, 195.
- ¹² S. Bessell, *Appl. Catal.*, 1995, 126, 235.
- ¹³ K. Góra-Marek, B. Gil, J. Datka, *Appl. Catal. A: Gen.*, 2009, 353, 117.
- ¹⁴ K. Góra-Marek, H. Mrowiec, S. Walas, *J. Mol. Struct.*, 2009, 923, 67.
- ¹⁵ S. Sklenak, P.C. Andrikopoulos, S. R. Whittleton, H. Jirglova, P. Sazama, L. Benco, T. Bucko, J. Hafner, Z. Sobalik, *J. Phys. Chem. C*, 2013, 117, 3958.
- ¹⁶ T. Iizuka, J. H. Lunsford, 1978, 100, 6106.
- ¹⁷ J. H. Lunsford, P. J. Hutta, M. J. Lin, K. A. Windhorst, *Inorg. Chem.*, 1978, 17, 606.
- ¹⁸ K. A. Windhorst, J. H. Lunsford, *J. Am. Chem. Soc.*, 1975, 97, 1407.
- ¹⁹ W. B. Williamson, J. H. Lunsford, *J. Phys. Chem.*, 1976, 80, 2664.
- ²⁰ K. Góra-Marek, *Vib. Spectrosc.*, 58 (2012) 104.
- ²¹ K. Góra-Marek, J. Datka, *Catal. Today*, 2011, 169, 181.
- ²² F. Bin, C. Song, G. Lu, J. Song, X.F. Cao, H.T. Pang, K.P. Wang, *J. Phys. Chem. C*, 2012, 116, 26262.
- ²³ F. Lónyi, J. Valyon, L. Gutierrez, M.A. Ulla, E. A. Lombardo, *Appl. Catal. B: Environ.*, 73, 2007, 1.

-
- ²⁴ F. Lónyi, H. E. Solt, J. Valyon, A. Boix, L. B. Gutierrez, *Appl. Catal. B: Environ.*, 212, 2012, 117.
- ²⁵ C.J. Van Oers, K. Góra-Marek, K. Sadowska, M. Mertens, V. Meynen, J. Datka, P. Cool, *Chem. Eng. J.*, 2014, 237, 372.
- ²⁶ R. Ahlrichs, H. Horn, A. Schaefer, O. Treutler, M. Haeser, M. Baer, S. Boecker, P. Deglmann, F. Furche. *Turbomole v5.9*, Quantum Chemistry Group, Universitaet Karlsruhe, Germany, 2006.
- ²⁷ M. Radoń, E. Broclawik, K. Pierloot, *J. Phys. Chem. B*, 2010, 114, 1518.
- ²⁸ E. Broclawik, A. Stepniewski, M. Radoń, *J. Inorg. Biochem.*, 2014, 136, 147.
- ²⁹ F. Neese, *J. Biol. Inorg. Chem.*, 2006, 11, 702-711.
- ³⁰ S.A. McMillan, L.I. Broadbelt, R.Q. Snurr, *J. Catal.*, 2003, 219, 117.
- ³¹ F. Göttl, J. Hafner, *J. Chem. Phys.*, 2012, 136, 64501
- ³² F. Göttl, J. Hafner, *J. Chem. Phys.*, 2012, 136, 64502.
- ³³ F. Göttl, J. Hafner, *J. Chem. Phys.*, 2012, 136, 64503.
- ³⁴ I. Georgieva, L. Benco, D. Tunega, N. Trendafilova, J. Hafner, H. Lischka, *J. Chem. Phys.*, 2009, 131, 54101
- ³⁵ P. Kozyra, M. Radoń, J. Datka, E. Broclawik, *Struct. Chem.*, 2012, 23, 1349.
- ³⁶ M. Radoń, P. Kozyra, A. Stepniewski, J. Datka, E. Broclawik, *Can. J. Chem.*, 2013, 91, 538.
- ³⁷ M. Radoń, E. Broclawik, *J. Phys. Chem. A*, 2011, 115, 11761.
- ³⁸ J. D. Henao, L. F. Córdoba, C. M. de Correa, *J. Mol. Catal. A: Chemical*, 2004 207, 195–204
- ³⁹ C.S. Pratt, B.A. Coyle, J.A. Ibers, *J. Chem. Soc. (A)*, 1971, 2146.
- ⁴⁰ Mercer, W.A. McAllister, J.B. Durig, *Inorg. Chem.*, 1967, 6, 1816.
- ⁴¹ M. Mitoraj, A. Michalak, *J. Mol. Model*, 2007, 13, 347.
- ⁴² M. Mitoraj, A. Michalak, T. Ziegler, *J. Chem. Theory Comput.* 5 (2009) 962.
- ⁴³ S. I. Gorelsky, E. I. Solomon, *Theor Chem Account*, 2008, 119, 57–65.
- ⁴⁴ A.-R. Allouche, *J. Comp. Chem.*, 32, 2011, 174.
- ⁴⁵ M. Radoń, (2011) *Natorbs* (v. 0.3) - a universal utility for computing natural (spin)orbitals and natural orbitals for chemical valence; <http://www.chemia.uj.edu.pl/~mradon/natorbs>. Accessed July 2014.

-
- ⁴⁶ J. Dědeček, Z. Sobalík, B. Wichterlová, *Catal. Rev.: Sci. and Eng.*, 2012, 54, 135.
- ⁴⁷ R. D. Feltham and R. S. Nyholm, *Inorg. Chem.*, 1965, 4, 1334.
- ⁴⁸ R. Bruce King (Ed.), *Encyclopedia of Inorganic Chemistry*, 1994, 2, 723.
- ⁴⁹ P. Kozyra, J. Załucka, M. Mitoraj, E. Broclawik, J. Datka, *Catal. Letters*, 2008, 126, 241.
- ⁵⁰ P. Rejmak, M. Mitoraj, E. Broclawik, *Phys. Chem. Chem. Phys.*, 2010, 12, 2321.
- ⁵¹ E. Broclawik, J. Załucka, P. Kozyra, M. Mitoraj, J. Datka, *J. Phys. Chem. C*, 2010, 114, 9808.
- ⁵² E. Broclawik, M. Mitoraj, P. Rejmak and A. Michalak, *Handbook of Inorganic Chemistry Research*, D.A. Morrison (Ed), Nova Science Publishers, Inc, New York USA, 201, 1361.
- ⁵³ E. Broclawik, J. Załucka, P. Kozyra, M. Mitoraj, J. Datka, *Catal. Today*, 2011, 169, 45.
- ⁵⁴ P. Kozyra, E. Broclawik, M.P. Mitoraj, J. Datka, *J. Phys. Chem C*, 2013, 117, 7511.

Ammonia-modified Co(II) sites in zeolites: IR spectroscopy and spin-resolved charge transfer analysis for NO adsorption complexes.†

Kinga Góra-Marek^{1*}, Adam Stępniewski², Mariusz Radoń¹ and Ewa Broclawik^{2*}

¹ *Faculty of Chemistry, Jagiellonian University in Kraków, Ingardena 3, 30-060 Krakow, Poland*

² *Jerzy Haber Institute of Catalysis PAS, Niezapominajek 8, 30-239 Krakow, Poland*

keywords: NO activation by Co(II) sites, ammonia co-adsorption, IR and DFT modeling, CT analysis

† **Electronic supplementary information (ESI) available:** Optimized geometries and the comparison of calculated charge and spin densities of $[\text{T1Co}(\text{NO})]^+$ and $[\text{T1Co}(\text{H}_2\text{O})_2(\text{NO})]^+$ models; Full list of geometric parameters calculated for studied systems; Comparison of relative energy calculated by various exchange-correlation functionals for singlet (\mathbf{b}_S) and triplet (\mathbf{b}_T) of $[\text{T1Co}(\text{NH}_3)_3(\text{NO})]^+$

* *corresponding author: kinga.goramarek@gmail.com*

* *corresponding author: broclawi@chemia.uj.edu.pl*

Abstract

IR spectroscopic studies and quantum chemical modeling (aided by the analysis of charge transfer processes between co-adsorbed ammonia and Co(II)-NO adduct) evidence that donor ammonia molecules, ligated to extraframework Co^{2+} centers in zeolites, vitally affect the strength of the N–O bond. Calculations indicate that versatility of ammine nitrosyl complexes, differing as well in the number of NH_3 ligands as in the geometry and electronic structure of Co-N-O unit (showing variable activation of NO) may co-exist in zeolite frameworks. However, only combined analysis of experimental and calculation results points to the adducts with three or five NH_3 coligands as decisive. The novel finding concerning the interpretation of discussed IR spectra is the assignment of the most down-shifted bands at $1600\text{-}1615\text{ cm}^{-1}$ to the N-O stretch in the singlet $[\text{Co}(\text{NH}_3)_3(\text{NO})]^{2+}$ adduct, in place of tentative ascription to pentaammine adducts. Theory indicates also that the Co(II) center (with manifold of close-lying electronic and spin states) acts as tunable electron donor where the spin state may open or close specific channels transferring electron density from the donor ligands (treated as the part of environment) to the NO molecule.

Introduction

Transition metal exchanged sites in porous materials invariably attract interest of researchers since strict limits imposed on NO emission triggered the development of various catalytic processes to limit pollution released to the atmosphere. Much attention is paid to the selective catalytic reduction (SCR), especially to the SCR with hydrocarbons (including otherwise inert methane).¹⁻³ Cobalt exchanged zeolites were found active in the latter process allowing for effective conversion of NO in oxygen-rich stream and in absence of undesired by-products like CO and N₂O.^{4,5} Favorable structure of the zeolite is frequently reported as very important for catalytic activity of cobalt sites; it is worth noting here that Co-ferrierites exhibit nearly doubled activity in the SCR process compared to Co-ZSM5 at T>500 Deg. C⁶ while the efficiency of Co-ZSM5 catalyst for decomposing NO in the presence of O₂ is one order of magnitude larger relative to Cu-ZSM5⁷. Co(II)-zeolites are also active in other reactions such as SCR of NO with NH₃^{8,9}, ammoxidation¹⁰, oxidation¹¹ or Fischer Tropsch synthesis¹². Therefore, the porous materials containing cobalt sites are still in the center of scientific interest, as well experimental as theoretical¹³⁻¹⁵.

Many factors may influence the overall activity of cobalt sites in zeolites towards NO, in particular the details of the interaction of NO with the adsorption center and the type of the formed bond can decide on both the path of the reaction and the transformation rate of adsorbed molecules. It is well known that unique properties of exchangeable transition metal ions (TMI), partially neutralized by basic oxygen ions from zeolite framework, are responsible for their high ability to activate π -electron molecules. However, neither the kind of an exchangeable transition metal cation or its location, nor the type of zeolitic structure and its chemical composition are the sole factors influencing the activation of the adsorbate. Already the early research by Lunsford *et al.* on nitrosyl complexes of cobalt and copper cations in A, X and Y zeolites has shown that co-ligated ammonia donated electrons upon

binding to the metal sites which activated NO and eventually led to nitric oxide reduction.¹⁶⁻¹⁹ Our former IR spectroscopic studies and quantum-chemical calculations have also indicated that other molecules of the strong electron donor properties ligated to the exchangeable TMI sites may vitally affect the activation of multiple bonds in the adsorbed molecules.^{20,21} It has been evidenced for the co-adsorption of carbon monoxide and organic/inorganic molecules (e.g. alkenes, aldehydes, ammonia, and pyridine) on the Cu⁺ center in zeolite CuZSM-5²⁰, and for ammonia and pyridine co-adsorbed with NO on CoZSM-5²¹. Although the latter studies concerned high-silica zeolites with structural properties different from those characteristic for Y zeolites, very similar effects have been registered. All these findings suggested that significant impact of the electron donor properties of co-adsorbed molecules on the weakening of multiple bonds might offer the opportunity for targeted bond activation.

In this work, IR studies on NO adsorption on ammonia-saturated CoMOR and CoFER zeolites are reported and supplemented by quantum chemical modeling in order to gain detailed insight into the influence of ammonia pre-adsorption on Lewis acidity of cobalt sites and the activation of NO. DFT calculations are done for a consecutive set of models mimicking a Co(II) site hosting as well NO as NH₃ ligands: Co(II)-NO and Co(II)(NH₃)_n-NO (with n = 3 or 5). The choice of the mononitrosyl model for Co(II) site interacting with NO is imposed by the presence of a well-isolated Co(II)-NO species, inferred in our group from the analysis of IR spectra recorded above 600 K for Co-ZSM5 zeolite²¹ while n values are based on experimental protocol. It has also been shown that the pre-adsorption of ammonia may lead to stable mononitrosyls even at room temperature while NH₃ co-adsorption significantly red-shifts the stretching frequency of mono-adsorbed NO.²² On the other hand, NO⁺ and NH₃ alone are also surface species of interest, postulated as conceivable key reaction intermediates of NO-SCR with CH₄ over Co-, (Co,Pt)- and H-mordenite catalysts^{23,24}.

Our former IR experiment²¹ and present results evidence strong red-shift of NO stretching frequency after ammonia pre-adsorption on the sample which implies that co-adsorption of NH₃ enhances backdonation from the cobalt site to NO ligand, in accordance with the work of Lunsford et al.¹⁶⁻¹⁹. Complementary quantum-chemical DFT modeling confirms that upon bonding of additional NH₃ molecules the red-shift of NO stretching frequency shows up; furthermore, the calculations show that the extent of NO activation strongly varies with the type of Co(II)-(NH₃)_n-NO adduct since it depends not only on the number of ammonia ligands, but also on the details of its electronic properties where spin state of the complex may have large effect on the activation ability of cobalt center towards NO. With regard to these findings we have undertaken explicit analysis of charge transfer processes between the co-adsorbed ammonia ligands and the Co(II)-NO core in adducts of various types (with the focus on their relation to donation/backdonation from/to NO antibonding orbitals) to better understand electronic mechanism behind the impact of strong donor co-ligands upon donor properties of the cobalt site.

2. Methods and Models

2.1 Experimental

The parent zeolites NaMOR (Si/Al = 6.5, ZEOLYST, CBV 10 A) and NaFER (Si/Al = 8.8, TOSOH) were ion-exchanged to their ammonium-forms NH₄MOR and NH₄FER. Hereto, the samples were stirred in a 0.5 M NH₄(NO)₃ - solution during 1 h at 353 K (100 mL NH₄(NO)₃ solution/g zeolite). After executing this procedure three times, the zeolites were washed and dried at 385K for 24 h. The ICP results confirmed that all Na⁺ cations have been exchanged. The NH₄MOR and NH₄FER zeolites were undergone the ionic exchange in 0.5M Co(NO₃)₂ solution at 353 K. After exchange procedure, samples were filtered and washed with water until the washing was free from nitrate ions, and dried at 385K for 24 h. The final

samples, designated as 'CoMOR' and 'CoFER', were characterized by an ICP method, revealing $\text{Co/Al} = 0.37$ and $\text{Co/Al} = 0.31$ for CoMOR and CoFER, respectively.

For IR studies a self-sustaining pellet of the sample was prepared, weighted and placed inside the IR cell. Prior to the measurements with the probe molecules, the samples have been degassed at 770 K for 1 h under high vacuum. In all studied cases ammonia (PRAXAIR 99.96%) was adsorbed in controlled amounts. To obtain maximum ligation of NH_3 molecules to Co^{2+} ions an excess of ammonia was adsorbed at 400 K, followed by an evacuation at the same temperature to remove the gaseous and physisorbed ammonia, which has been tracked by the recording of spectra. Subsequently, the FT-IR spectrum was taken at room temperature. The concentration of Lewis sites was calculated using respectively the intensities of the 1620 cm^{-1} band of ammonia coordinatively bonded to Lewis sites (NH_3L) by applying its extinction coefficient. The extinction coefficient of $0.026 \text{ cm}^2 \mu\text{mol}^{-1}$ for the NH_3L band was determined in experiments in which ammonia was adsorbed in dehydroxylated zeolite HY (pre-treated at 1070 K), containing Lewis acid sites as main species.²⁵ Even if the 1620 cm^{-1} band could be due to ammonia interacting with Lewis sites of different nature, i.e. Al- (in dehydroxylated zeolite HY) or Co-Lewis ones (in zeolite under the study), the same value of the extinction coefficient was assumed based on the same value of the $\text{NH}_3\text{-Co}$ and $\text{NH}_3\text{-Al}$ band frequencies. In zeolites under the study only Co^{2+} cations can be considered as Lewis acid sites: neither Na^+ sites nor Al-Lewis sites originated from dehydroxylation were detected. Consequently, the amount of ammonia pre-adsorbed was divided by the number of Co^{2+} cations derived from ICP analysis. For zeolites fully saturated with ammonia the presence of $[\text{Co}(\text{NH}_3)_5]^{2+}$ pentaamminenitrosylcobalt(II) complexes was confirmed. Following the same rule, the $[\text{Co}(\text{NH}_3)_3]^{2+}$ triamminenitrosylcobalt(II) were immobilized in zeolite CoMOR and CoFER. In this case, ammonia was introduced to IR cell in controlled and measured doses up

to the intensity of the 1620 cm^{-1} band of ammonia coordinatively bonded to Co^{2+} sites attained the value corresponding the ratio $3\text{ NH}_3/\text{Co}^{2+}$.

Zeolites hosting both $[\text{Co}(\text{NH}_3)_5]^{2+}$ and $[\text{Co}(\text{NH}_3)_3]^{2+}$ were subjected to the sorption of nitrogen oxide (Linde Gas Polska 99.5%). Sorption of the doses of NO was performed at room temperature up to the appearance of the rotation-vibration bands of gaseous NO. Such procedure assured the reaction of NO molecules with all $[\text{Co}(\text{NH}_3)_5]^{2+}$ and $[\text{Co}(\text{NH}_3)_3]^{2+}$ complexes immobilized in studied zeolites. Consequently, the spectra discussed in this work show the maximum intensities of all NO bands appeared after NO adsorption in zeolites with pre-adsorbed ammonia.

The IR spectra were recorded at room temperature with a Bruker Tensor 27 spectrometer (equipped with an MCT detector) with the spectral resolution 2 cm^{-1} .

2.2 DFT calculations

Geometrical and electronic structure optimizations for studied cluster models were performed by means of Turbomole 5.9²⁶ software within UDFT (unrestricted density functional theory) method with the BP86 exchange–correlation functional and the def2-TZVP basis set provided by the Turbomole package. For discussion of the singlet – triplet splitting we also tested other exchange–correlation functionals (see below).

The performance of the BP86 functional for open-shell adducts between late TM centers and the radical NO ligand has been previously tested by us by comparing selected DFT methods with accurate correlated methods for Fe(II) complexes with NO (in heme and non-heme architectures).^{27,28} It was found that for these $\{\text{Fe-NO}\}^7$ systems, the non-hybrid functionals, like BP86, best reproduced spin density distributions from the multiconfigurational CASSCF approach; importantly, these functionals avoid an excessive spin polarization characteristic of the hybrid functionals. Furthermore, selected iron

complexes, $[\text{Fe}^{\text{II}}(\text{H}_2\text{O})_5(\text{NO})]^{2+}$ and $\text{Fe}^{\text{II}}\text{P}(\text{NH}_3)\text{NO}$, were successfully analyzed in terms of the nature of Fe-NO bond within SR-NOCV (spin-resolved natural orbitals for chemical valence) method, using the DFT/BP86 calculation scheme.²⁸ Moreover, non-hybrid functionals, including BP86, even if imperfect for the energetics, are known to give reliable molecular structures and harmonic frequencies.²⁹ BP86 functional has also been used to evaluate thermodynamics of adsorption of NO on cobalt as a function of the local environments in ferrierite zeolites.³⁰ Recently, a thorough investigation of NO adsorption in Co(II)-exchanged CHA, MOR, and FER zeolites, based on periodic calculations initiated in the group of Hafner,^{15,31-34} also indicated that as well electronic as vibrational properties of Co(II) sites and their mono- and dinitrosyl complexes were predicted with satisfactory accuracy by the non-hybrid functionals.

All these results corroborated our pre-assumption that BP86 functional is a good choice for describing the electronic structure of NO complexes with open-shell cations in a zeolite, including non-innocent $\{\text{Co-NO}\}^8$ systems. Since this work focuses on the impact of electron density deformation upon coordination of additional donor ligands by Co(II) centers onto properties of the NO bond, we base the selection of computational protocol on the performance of BP86 functional with respect to reproducing total electron and spin densities. To this end, some additional tests of the performance of DFT/BP86 method against other functionals, with respect to reproducing spin density and electronic structure from CASSCF calculations (practical with reasonable active space for the minimal conceivable model of the site) have been performed. Detailed studies on the energetic and electronic properties of cobalt complexes with NO by correlated wave function methods are under way in our group and will be published in due time.

Elementary cluster model for the Co(II) site in a zeolite used in this work is based on the simplest conceivable mimic of the framework, e.g. on a single $\text{Al}(\text{OH})_4^-$ tetrahedron

(labeled hereafter as T1). We have already used such model to successfully discriminate between donor properties of Cu(I) and Cu(II) sites in zeolites towards NO.^{35,36} The same model has also been used by us in the CASSCF/CASPT2 studies on mono and dinitrosyls on copper sites in zeolites.³⁷ However, since multiple coordination of Co with the framework should be assumed for majority of zeolitic sites³⁰⁻³⁴, our working model for the Co(II) site is extended here by including two additional water ligands to cobalt to crudely restore fourfold coordination of Co(II) center to basic oxygens. The water ligand as the simplest mimic of a coordinate bond with the basic oxygen has already been used in early modeling studies of cobalt sites.^{30,38} The model proposed here is not neutral, however, we believe that the screening of its effective +1 charge by negative zeolite framework shall merely shift the calculated frequencies, leaving the relative shifts reasonably estimated (see also section 3.3 Vibrational analysis). The minimal cluster applied in our modeling obviously does not allow to discriminate between various zeolite types or cobalt siting; we are fully aware of this shortcoming when relating specific calculation results to experimental data averaged over site speciation.

As compared with bare [(T1)CoNO]⁺ model, addition of two water ligands in the proposed [(T1)Co(H₂O)₂NO]⁺ model somewhat modified Lewis properties of the cobalt center. As expected, the charge on Co cation became slightly more neutralized while the bonding with NO remained essentially unchanged which manifested in negligible shift of NO stretching frequency (by 1.5 cm⁻¹). The improvement due to better mimicking the coordination of the Co²⁺ center manifested in a better localization of spin and electron density on the cobalt in T1Co⁺ fragment. The comparison of geometries, atomic charges and spin densities for [(T1)CoNO]⁺ and [(T1)Co(H₂O)₂NO]⁺ (**a**) is given in ESI. Further studies on the effect of extending cluster models for pertinent cobalt sites (eventually periodic calculations) are under way in our group.

In addition to the primary cluster model $[(T1)Co(H_2O)_2NO]^+$ (**a**) for the adduct of NO with the parent Co(II) site, we consider two model systems for NO adsorption on ammonia-saturated cobalt zeolite: $[(T1)Co(NH_3)_3NO]^+$ (**b**) and $[Co(NH_3)_5NO]^{2+}$ (**c**). We introduce the (**b**) and (**c**) models following the IR experimental results (see section 3.1), suggesting the average numbers of NH_3 ligands coordinated to a single Co(II) site under specified saturation condition as three or five, respectively. Here we assume that the coordination of three strongly bonded ammonia ligands in (**b**) displaces two basic oxygens (simulated in the model by water molecules), while the fivefold ammonia coordination in (**c**) entirely hinders the bonding with the framework. Structure (**c**) as well offers the model for the ammonia-only species proposed on the basis of IR spectrum in fully ammonia-saturated CoMOR zeolites (*vide infra*) as corresponds to the black isomer of pentaamminenitrosylcobalt(II) dichloride^{39,40}.

2.3 SR-NOCV analysis

SR-NOCV (spin-resolved natural orbitals for chemical valence) method^{41,42} is the extended charge decomposition analysis to investigate the electronic relaxation accompanying the formation of a bond between the fragments of the complex system. Complementary alternative schemes based on population analysis of fragment orbitals have also been proposed in the literature,⁴³ however, we continue our study within NOCV methodology where we have already gained expertise in the field of NO bonding to transition metal centers^{28,35,36}. Our previous studies on the interaction of NO with transition metal sites have successfully invoked spin resolution which appeared indispensable to bring novel particulars to the charge transfer analysis, related to the non-innocence of the open-shell NO ligand.

SR-NOCV analysis decomposes the differential density (the difference between electron densities of the final complex and the promolecule) into one-particle contributions, separately for α and β spins. The corresponding promolecule (taken in the geometry of the complex) for each considered system is built of the respective two non-interacting fragments;

herein: the co-adsorbed NH_3 ligands and the Co(II)-NO core, because this work is focused on the influence of ammonia on the bonding within the Co(II)-NO unit. Single point UDFT calculations are performed for the respective fragments in order to compute the differential electron density for each complex. Its diagonalisation provides NOCV orbitals. The pair of the corresponding NOCVs (linked by the modulus of eigenvalues, where the orbital with negative eigenvalue depicts the decrease, and that with positive eigenvalue – the increase of electron density) defines an electron transfer channel between the NH_3 molecules and the Co(II)-NO core. The eigenvalue offers a measure for electron density transferred along a particular charge transfer channel, while the plot visualizes the pathway of electron density transfer (from the region depleted to the region enriched in electron density). Plots are generated with the Gabedit software⁴⁴ from the output of home-made program Natorbs⁴⁵ serving to calculate the NOCV orbitals.

3. Results and Discussion

3.1 IR spectra

The sorption of NO at room temperature in zeolites CoMOR and CoFER have resulted in the formation of dinitrosyl complexes $[\text{Co}(\text{NO})_2]^{2+}$ as the most stable species (Figure 1). Generation of mononitrosyls $[\text{Co}(\text{NO})]^{2+}$ (the species of the lower stability) required thermal decomposition of the dinitrosyls $[\text{Co}(\text{NO})_2]^{2+}$ at 330 °C (Figure 1). Only in such experimental conditions the $[\text{Co}(\text{NO})]^{2+}$ band at ca. 1845 cm^{-1} was detectable. The comparison of the N-O stretching frequency in the mononitrosyl adducts $[\text{Co}(\text{NO})]^{2+}$ (ca. 1850 cm^{-1}) to the gaseous NO (1875 cm^{-1}) evidences a minor activation of NO molecule by Co^{2+} ions bonded to framework oxygen atoms ($\Delta\nu = 25 \text{ cm}^{-1}$) (Table 1).

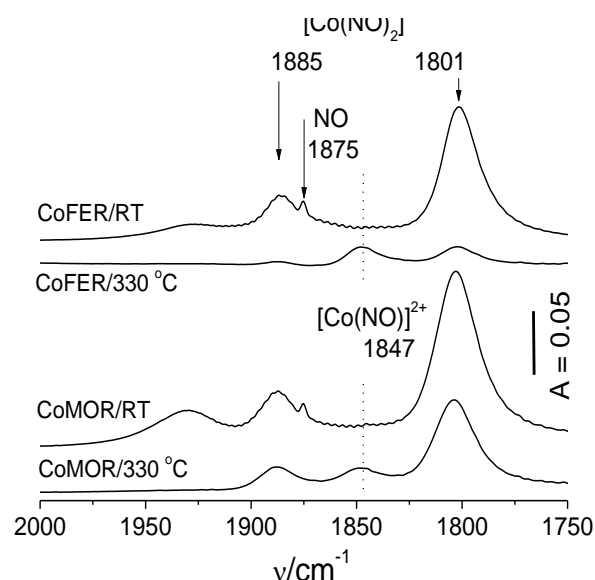


Fig. 1. The spectra of NO adsorbed at room temperature and at 330 °C in zeolites CoFER and CoMOR.

Other series of experiments was designed to evidence the impact of ammonia ligated to the exchangeable Co^{2+} cation on the NO bond. To this end, NO was sorbed in zeolites CoMOR and CoFER with controlled amounts of pre-adsorbed ammonia. Sorption of the measured doses of ammonia in zeolites led to in the appearance of the 1620 cm^{-1} band of NH_3 bonded coordinatively to cationic sites, $\text{H}_3\text{N-Co}^{2+}$. After adsorption of consecutive ammonia doses, the intensity of the 1620 cm^{-1} band (due to H-N-H bending) was measured and used to evaluate the average number of ammonia molecules interacting with one Co^{2+} cation. The value of the applied extinction coefficient was typical of the Al-originated Lewis sites ($0.026\text{ cm}^2\mu\text{mol}^{-1}$)²¹. Even if the 1620 cm^{-1} band could be due to ammonia interacting with Lewis sites of different nature, i.e. Al- or Co-Lewis ones, the same value of the extinction coefficient was assumed based on the same value of the $\text{NH}_3\text{-Co}$ and $\text{NH}_3\text{-Al}$ band frequencies. In this way, the average numbers of NH_3 molecules interacting with one Co^{2+} cation in distinct samples have been evaluated as 3 NH_3/Co and 5 NH_3/Co , respectively (depending on the zeolite and sample type).

The sorption of NO in CoMOR and CoFER zeolites treated with the dose of ammonia corresponding to three NH₃ per Co²⁺ site (*vide supra*) has evidenced a significant red shift of the NO band attributed to the formation of the [Co(NH₃)₃(NO)]²⁺ complexes. Analysis of the differential spectrum of NO sorbed in CoMOR zeolite accommodating [Co(NH₃)₃]²⁺ adducts has revealed the development of two mononitrosyl [Co(NH₃)₃(NO)]²⁺ bands (1765 and 1745 cm⁻¹) pointing to the heterogeneity of Co(II) siting⁴⁶ with variable neutralization of the positive charge of Co²⁺ cations in the [Co(NH₃)₃(NO)]²⁺ adducts (Figure 2, spectrum a). For zeolite CoFER only one band at 1730 cm⁻¹, assigned to [Co(NH₃)₃(NO)]²⁺ complex (Figure 2, spectrum b) has been identified. In general, a vital feature of NO in [Co(NH₃)₃(NO)]²⁺ adducts is the significant downshift of N-O vibration with respect to the frequency of NO in the gas phase ($\Delta\nu = 130\text{-}110\text{ cm}^{-1}$). It indicates that the NO bond in the Co(NH₃)₃(NO)]²⁺ complexes is substantially weakened. The presence of the 1750 cm⁻¹ band has additionally been reported for zeolite CoZSM-5²¹ where it was tentatively assigned to the mononitrosyls with four NH₃ ligands. The weakening of N-O bond, evidenced by the significant red shift, may be related to the back donation of electrons from basic ammonia molecules *via* Co²⁺ to antibonding π^* orbitals on NO molecule. Assuming the same number of NH₃ molecules per Co site (i.e., 3), i.e., the existence of [Co(NH₃)₃(NO)]²⁺ complexes in both MOR and FER zeolites, different π^* -backdonation ability of Co²⁺ cations in these zeolites can be assigned to variable speciation of cobalt sites in these zeolites, including Si/Al ratio, site location or geometric features of the framework. All these factors could lead to variable extent of the neutralization of Co²⁺ cations by the negative framework; theoretical modeling at molecular level has been undertaken in the hope to partially unravel determinants influencing the status of the cobalt center.

Moreover, for both MOR and FER zeolites the presence of significantly red shifted band at 1615 cm⁻¹ was also detected. In the light of quantum chemical calculations (presented

in sections 3.2) as well the band at ca. 1615-1610 cm^{-1} as that at 1765-1730 cm^{-1} can be assigned to the $[\text{Co}(\text{NH}_3)_3(\text{NO})]^{2+}$ species in alternated electronic (in particular spin) states.

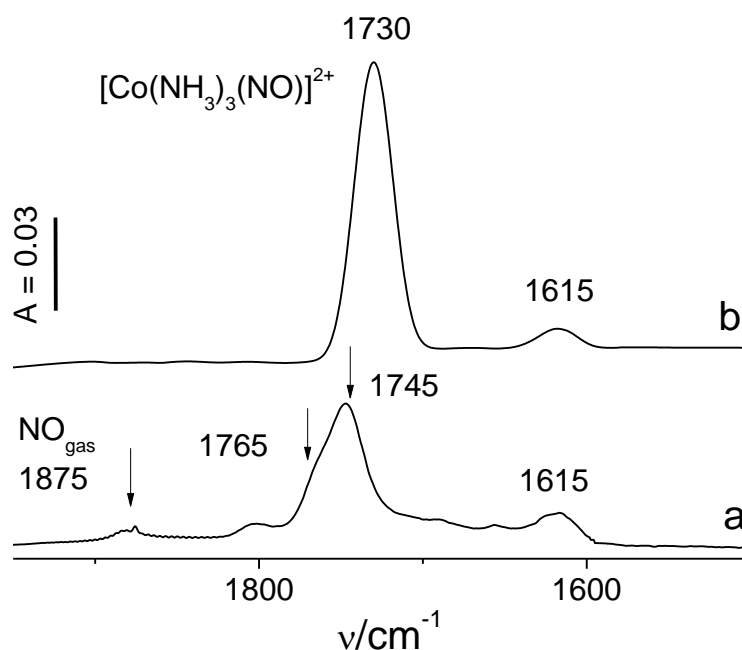


Fig. 2. The spectra of NO adsorbed in zeolites CoMOR (a) and CoFER (b) hosting the $[\text{Co}(\text{NH}_3)_3]^{2+}$ complexes

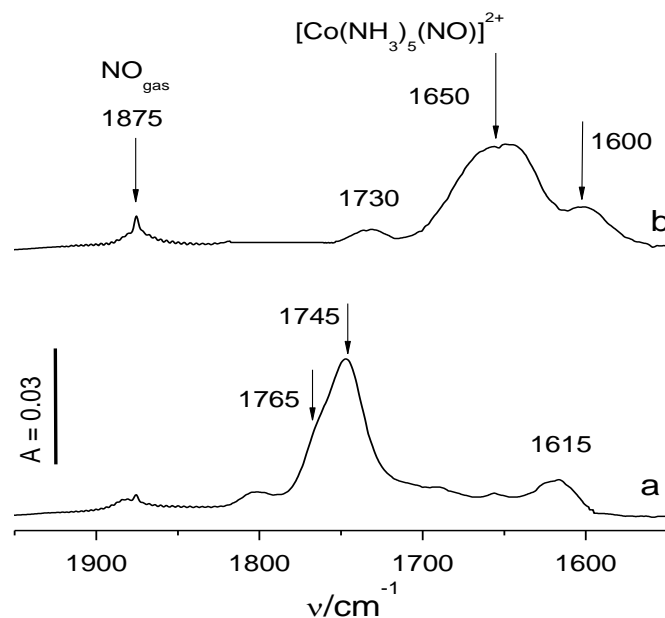


Fig. 3. The spectra of NO adsorbed in zeolite CoMOR accommodating $[\text{Co}(\text{NH}_3)_3]^{2+}$ (a) and $[\text{Co}(\text{NH}_3)_5]^{2+}$ complexes (b).

The sorption of NO was also performed in CoMOR zeolite pretreated with the highest doses of ammonia and presumably hosting the $[\text{Co}(\text{NH}_3)_5]^{2+}$ pentaammine complexes, i.e. holding Co^{2+} cations nearly saturated by ammonia molecules. The sorption of NO has resulted in appearance of the complex band centered at 1650 cm^{-1} , the origin of which are immobilized immobilized pentaamminenitrosylcobalt(II) complexes (Figure 3, spectrum b). A weak band around 1600 cm^{-1} is also noticeable for these samples. The $[\text{Co}(\text{NH}_3)_5(\text{NO})]^{2+}$ complexes are widely known in the cobalt coordination chemistry and usually regarded as NO^- complexes of Co(III). In such $[\text{Co}^{\text{III}}(\text{NH}_3)_5(\text{NO}^-)]^{2+}$ complexes complete electron transfer from Co^{2+} to NO was postulated: the Co^{3+} oxidation state is stabilized by NH_3 and other electrodonor ammonia ligands, as well as by CN^- in $[\text{Co}(\text{CN})_5(\text{NO})]^{3-}$ complexes. The very low frequency for the NO stretching vibration when NO gains electron density has been commonly accepted;^{43,44} for these compounds the +3 oxidation state has been attributed to the cobalt and the NO stretching frequency was assigned to the bands between 1550 and 1650 cm^{-1} .^{47,48} In consequence, very strong impact of the electron donor properties of co-adsorbed molecules on the weakening of multiple bonds should provide the opportunity for targeted N-O bond activation.

It should be additionally noted that the $[\text{Co}(\text{NH}_3)_5(\text{NO})]^{2+}$ complexes have been formed in zeolite CoFER only in negligible quantities. While mordenite is considered as a 12-ring structure, ferrierite is only a 10-ring zeolite, thus the framework topology restrictions may be responsible for the absence of bulky $[\text{Co}(\text{NH}_3)_5(\text{NO})]^{2+}$ complexes.

3.2 Structural and electronic properties of cluster models

Optimized structures of the studied models (a) – (c) are shown in Fig. 4. We examine in detail the triplet state for (a) and the singlet for (c). For the parent Co(II) site we follow suggestions inferred from former works³⁰⁻³⁴ where a spin of $S = 1$ in Co(II) sites and their adducts with nitrosyl, arising from localized spins with opposite orientations on the high-spin

Co cation and the NO ligand was proposed. Nevertheless, the singlet state for **(a)** was also tested but as well the geometry, electronic and vibrational properties as the energetic separation from the ground-state triplet indicates that both structures are nearly equivalent. The comparison of the Co-O bond lengths with periodic models studied by Göttl et al.³¹⁻³⁴ shows that the cluster model $[(T1)Co(H_2O)_2NO]^+$ **(a)** reasonably mimics the bonding with four framework oxygens (compare the distances of 2.19, 2.19, 1.97 and 1.97 Å in cluster model to the distances in the range of 1.85 to 2.36 Å obtained by DFT/PBE in periodic models, depending on the cobalt siting). Next, ammonia ligands were consecutively added, constituting ammonia-saturated **(b)** and **(c)** adducts. Furthermore, we assume that five strongly interacting ammonia ligands suppress the spin on cobalt cation to the low-spin state in **(c)**; additional arguments in favor of the singlet come from the comparison of geometric parameters calculated for the singlet complex **(c)** with experimental crystal structure of pentaamminenitrosyl cobalt(II) dichloride (*vide infra*). In variance, for the intermediate **(b)** model with three coordinated NH_3 ligands as well the singlet (S) as triplet (T) spin states are scrutinized for further analysis since these two states show very distinct geometric and vibrational properties while being very close in energy. Full listing of structural parameters for the triplet **(a)**, the singlet **(c)**, and singlet and triplet states **(b_S)** and **(b_T)**, along with the comparison of singlet-triplet splitting for **(b)** calculated by various exchange-correlation functionals are given in ESI. Table 2 lists selected geometric parameters relevant for NO activation (the Co-N-O angle, Co-N and N-O distances) for models **(a)**, **(b_S)**, **(b_T)** and **(c)**.

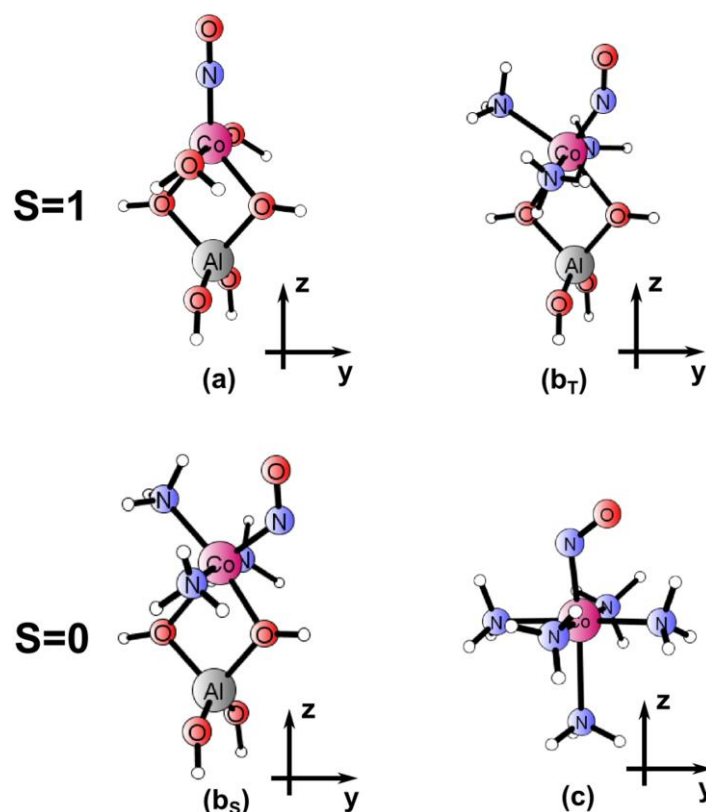


Fig. 4. DFT-optimized structures of triplet models for NO adducts with Co(II) sites: with no ammonia (parent model **(a)**, GS), three ammonia co-ligands (**(b_T)**) and of singlet models for three (**(b_S)**) or five (pentaamminenitrosylcobalt(II) (**(c)**, GS) ammonia co-ligands

Model **(a)** (Figure 4(a)) has a linear Co-N-O motif and is used as a reference to analyze the NO bonding by a non-modified cobalt site. For the complex with three ammonia ligands, the singlet adduct (**(b_S)**) has a strongly bent Co-NO unit (122°), while the triplet structure (**(b_T)**) shows a moderate bend of the Co-N-O motif (148°). In the case of the singlet **(c)** adduct the coordination of five ammonia ligands (hindering the bonding of cobalt cation to the zeolite fragment) makes the Co-N-O unit strongly bent. The two spin states in the **(b_S)** and **(b_T)** complexes are nearly degenerate in energy. The BP86 functional points to the singlet lying only 5.2 kcal/mol below the triplet but the energy difference (and even its sign) are strongly functional-dependent (the comparison with other GGA and hybrid functionals is given in ESI). Hence we conclude here that both spin states may coexist in reality.

Furthermore, in order to test reliability of the assumption that the coordination with strong ammonia donors may compete with additional Co-O bonds to the framework, we have calculated the energy gain while going from complex **(a)** to complex **(b_T)**. The exchange of two water ligands by two NH₃ ligands (an intermediate stage to the formation of **(b)**, with very similar structure to that of [(T1)Co(H₂O)₂NO]⁺ one) is exothermic by as much as 22.5 kcal/mol. Addition of the next ammonia ligand to give **(b_T)** still lowers the energy (by another 22.2 kcal/mol). In view of the well-known strong dependence of the calculated adsorption energies on the choice of exchange-correlation functional we have additionally inspected this aspect. Tests with B3LYP functional evidenced that in the cobalt case the dependence was not dramatic: the exchange of water by ammonia ligands yielded energy gain by 16.6 kcal/mol while the addition of the third ammonia ligand yielded the energy gain by 21.8 kcal/mol.

Detailed analysis of the spin density for model complexes brings an interesting insight into their electronic structure. Spin density distribution for complex **(a)** (shown in Fig. 5a) confirms that the triplet spin state stems from an antiferromagnetic coupling of the quadruplet Co²⁺ (with the occupations $d_{xy}^2 d_{yz}^2 d_{xz}^{\uparrow} d_{z^2-x^2}^{\uparrow} d_{y^2}^{\uparrow}$) with the unpaired electron on the NO ligand (π_x^{\downarrow}). This interpretation agrees with that discussed in ref. 33; however, it must be stressed here that due to cylindrical symmetry of the Co-N-O unit, the actual electronic structure of the complex should involve the second equivalent configuration, namely $d_{xy}^2 d_{yz}^{\uparrow} d_{xz}^2 d_{z^2-x^2}^{\uparrow} d_{y^2}^{\uparrow}$, antiferromagnetically coupled to π_y^{\downarrow} on NO. Therefore, fully correct description of this complex would call for multiconfiguration wavefunction methodology and such a study is under way in our group.

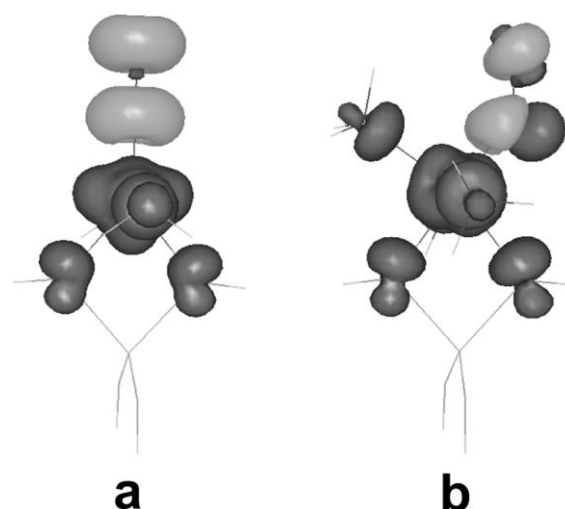


Fig. 5. Spin densities for triplet complexes: $[(T1)Co(H_2O)_2NO]^+$ (a) and $[(T1)Co(NH_3)_3NO]^+$ (b); dark grey – majority spin, light grey – minority spin, contour value of 0.003.

For the triplet complex comprising three ammonia ligands (**b_T**), the spin distribution (shown in Fig. 5b) also suggests an electronic configuration, inferred from the quadruplet cobalt cation (with the occupations $d_{xz}^2 d_{\perp}^2 d_{\parallel}^{\uparrow} d_{x^2-y^2}^{\uparrow}$) antiferromagnetically coupled to $\pi_{\parallel}^{*\downarrow}$ on NO. Due to rotation of the axis pointing along the Co-N bond, the notation d_{\parallel} and d_{\perp} (with respect to the Co-N-O plane) is used here. The major difference between the two triplet states is related to the bent geometry of the Co-N-O unit in the latter, which enables a weak σ coupling between the d_{\parallel}^{\uparrow} and $\pi_{\parallel}^{*\downarrow}$ orbitals, and makes the empty π_{\perp}^* on NO ready for backdonation from doubly occupied cobalt d_{\perp} orbital. The two singlets, (**b_S**) and (**c**) have closed shell electronic structure attributable to the configuration $d_{xz}^2 d_{\perp}^2 d_{yz}^2 \sigma_{Co-NO}^2 d_{x^2}^0 \pi_{\perp}^{*0}$. Here again, the strongly bent NO geometry is favorable for making a strong σ bond as well as for significant backdonation from the doubly occupied d_{\perp} to the empty π_{\perp}^* on NO. These electronic parameters may be related to the activation of NO bond evidenced by IR red shift of its stretching frequency (as discussed in the following paragraphs).

Only in the case of complex (**c**) structural parameters may be compared to the measured crystal structure of $[Co(NH_3)_5NO]^{2+}$ cation in pentaamminenitrosylcobalt(II)

dichloride.³⁹ The comparison of calculated and experimental structural data (see Table 2) indicates good agreement with the crystal structure which may be taken as an indirect experimental support in favor of the singlet ground state for the black isomer of this complex.

3.3 Vibrational analysis

Table 3 compares the values of NO stretching frequency calculated for NO interacting with models mimicking various Co(II) sites (in non-modified or ammonia-saturated zeolites) with the measured ones (averaged over zeolite types and site speciation for the bands). The assignment of the models to IR bands registered for $[\text{Co}(\text{NH}_3)_3(\text{NO})]^{2+}$ and $[\text{Co}(\text{NH}_3)_5(\text{NO})]^{2+}$ adducts is based on scrutinized re-inspection of experimental spectra in the context of the closest correspondence between the calculated and measured frequencies and is given in the second column (cf. section 3.1). Our detailed analysis suggests that the most red-shifted NO band does not correspond to the highest number of ammonia ligands, but to the intermediate saturation with three donor ligands per site, albeit with the spin on the cobalt cation reduced from the quadruplet (in the parent Co(II) site) to the doublet. The singlet state for the complex comes from the coupling of Co^{2+} ($S=1/2$) with the unpaired electron on NO. The same resultant singlet spin state emerges for pentaamminenitrosyl Co(II) complex, but both calculated and measured red-shifts are lower than for the singlet adduct with three NH_3 ligands. Table 3 lists also the calculated total charge and spin densities on the adsorbed NO. It is clear that co-adsorption of electron-donating ammonia ligands substantially red-shifts stretching frequency of NO which is evidenced as well by the experiment as by the calculation; however, only DFT modeling revealed that the extent of NO activation critically depends also on particulars of the electronic structure (e.g. spin state) of the adduct. In view of the limitations put on the accuracy of calculation results by the simplified, positively charged cluster model and harmonic approximation, the overall agreement of theoretical results with the trends observed in experiment is acceptable. Larger error in the case of model

(c) may be ascribed to complete negligence of charge screening due to the embedding in electron-rich zeolitic environment; the source of error with respect to the actual amminitrosylcobalt(II) dichloride may be rooted in other factors, e.g. negligence of nearest neighbors in the crystal lattice. For the parent complex (a) the calculations give blue-shift instead of a minute red-shift in the experiment; however, this effect is already well-known from previous studies where these shifts in the range of $+57 \div +86 \text{ cm}^{-1}$ were found with equivalent GGA PBE functional for periodic models of real zeolites^{15, 33, 34}.

The calculated red-shift of the NO stretch due to ammonia co-ligation is generally underestimated (by 24 to 41 cm^{-1}) with respect to the experiment but the trend in shifts attributed to additional ammonia co-ligands is reasonably reproduced. The most important observation is that theory predicts versatility of possible forms for the $[\text{Co}(\text{NH}_3)_n(\text{NO})]^{2+}$ adducts, diverse not only by the number of ammonia molecules, but also by the spin state and by the geometry of Co-N-O unit. The energy separation between spin states is small and strongly functional-dependent (the singlet is generally favored for ammonia-ligated adducts by the DFT/BP86 calculation), thus it may be rather suggested that various forms may coexist in real zeolites and under ambient conditions. In consequence, only the ranges of experimental frequency red-shifts may be used as the reference to calculation since the emergence of selected distinct forms may depend on the zeolite type and on experimental conditions (not accounted for by the present small models). Earlier DFT calculations for periodic models of NO adsorption on cobalt sites in chabazite, mordenite, and ferrierite zeolites^{15, 30, 33, 34} also pointed to the existence of diversity of NO adducts in the zeolite framework, showing different geometries and frequencies.

Nevertheless, the novel finding concerning the interpretation of the discussed IR spectra (stemming from DFT modeling) is the proposal to assign the most down-shifted bands

at 1600-1615 cm^{-1} rather to the singlet state of $[\text{Co}(\text{NH}_3)_3(\text{NO})]^{2+}$ adduct than to a feature belonging to the spectrum of pentaammine adducts (released to the cavity, the latter practicable in selected zeolite types with sufficiently large cavities). This could not be foreseen without scrutinized calculations.

In addition to the calculated stretching frequencies, theoretical modeling gives also specific information not accessible from the experiment, such as geometrical parameters (Table 2) and electron or spin populations on NO ligand (Table 3), presumably evidencing donation/backdonation processes. Unfortunately, neither of these descriptors satisfactorily correlates with the absolute red-shift of NO stretching frequency (either measured nor calculated). Even if some crude relation of the red shift to the bending of NO unit and diminishing of positive charge on NO might be noticed, neither the charge nor spin density on NO fully rationalizes the postulated occurrence of strong backdonation.

3.4 Interpretation of SR-NOCV analysis

In our former papers we have already postulated that the analysis of independent electron density flow channels (depicting virtual charge transfer processes) was able to properly identify the source of ligand activation.^{28,35,36,49-54} Therefore, in order to quantify the influence of additional donor ligands to the cobalt center on its donation/backdonation ability, for the complexes with three ammonia ligands (in singlet and triplet states, \mathbf{b}_S and \mathbf{b}_T) and with five ammonia ligands (\mathbf{c}) we have scrutinized the analysis of the differential density (calculated for the promolecule built from ammonia ligands shell as the one fragment and the remainder of the Co(II)-NO core as the other fragment). Since the spin on the closed-shell fragment corresponding to the ammonia ligands is always singlet, the spin on the other fragment is unambiguously set to the singlet for (\mathbf{b}_S) and (\mathbf{c}), and to the triplet for (\mathbf{b}_T). The dominant orbital and spin resolved charge transfer channels (defined by the NOCVs with an

eigenvalue modulus larger than the threshold of 0.1), serve here to quantify the transfer of electron density from the NH_3 lone pairs to the Co(II) center and to the NO ligand.

We recall that the three models, (**b_S**), (**b_T**) and (**c**), subjected to the analysis, have been found in section 3.3 to present interestingly distinct vibrational properties: the triplet $\text{Co(II)(NH}_3)_3(\text{NO})$ adduct (**b_T**) reproduces the red shift of NO stretching frequency corresponding to the IR band routinely attributed by experiment to three NH_3 molecules ligated to Co(II) site, whereas its singlet counterpart (**b_S**) offers strikingly distinct activation ability and, unexpectedly, reproduces the most red-shifted IR band, formerly overlooked in experimental studies. Model (**c**) reproduces the properties of the pentaammine cobalt adduct invoked in experimental interpretation of IR spectrum for fully ammonia-saturated cobalt zeolites.

The resultant NOCV independent charge flow channels, plotted according to the convention ascribing red contours to the depletion and blue contours to the gain of electron density, are shown in Figures 6 and 7 for the models in the triplet or the singlet state, respectively. We can interpret each channel as corresponding to the electron flow upon the bond formation from the red area to the blue region. The corresponding eigenvalue is given together with the contour plot for each channel and serves for estimating the number of electrons redistributed along this channel (i.e., to quantify its efficiency in the total charge transfer between the fragments). The assumed partition scheme allows direct visualizing the influence of ammonia co-adsorption on the electron density redistribution within the Co-N-O core by inspecting resulting charge flow channels between NH_3 ligands and the remainder of a particular model. Figures 6 and 7 show solely the selected channels, characterizing the influence of ammonia co-ligation on the NO bond.

Fig. 6 shows spin-resolved channels for the triplet (\mathbf{b}_T) model. Only one channel (in spin majority manifold, with the eigenvalue of 0.46), describes the effective flow of α electron density from three ammonia lone pairs to NO. The corresponding channel for β spin manifold depicts merely density flow from ammonia lone pairs to the cobalt center without participation of NO ligand, and thus it is assumed here not directly related to NO activation. In variance, for the two singlet structures (\mathbf{b}_S) and (\mathbf{c}), Fig. 7) there are two cumulative ($\alpha+\beta$) channels with large eigenvalues .

Since the eigenvalues quantify the channel efficiency (i.e. the amount of transferred electron density) these channels may be directly taken as the signature of the increase in backdonation ability of the site to the antibonding π^* orbital on NO and thus its activation propensity towards NO. In summary, after ligation of ammonia molecules to the cobalt center significant transfer of electron density from donor ligands via the Co(II) core to the antibonding orbital on NO ligand shows up, which nicely corroborates the experimental interpretation of relevant IR spectra. However, its quantitative ratio and thus the expected effect on the NO bond activation depends not only on the number of donor ligands, but also on the spin state of the system. This suggests that the particulars of the electronic structure of the Co(II) center may play a vital role in opening or closing specific electron transfer channels between the site and NO ligand.

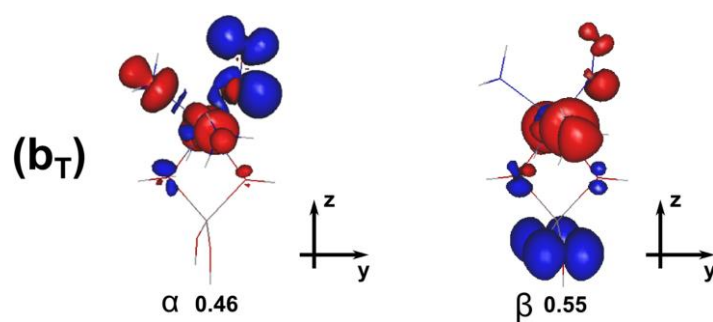


Fig.6. Dominant spin-resolved (α or β) electron transfer channels for the triplet (**b_T**) model with corresponding eigenvalues (blue: accumulation, red: electron density depletion; contour value 0.001)

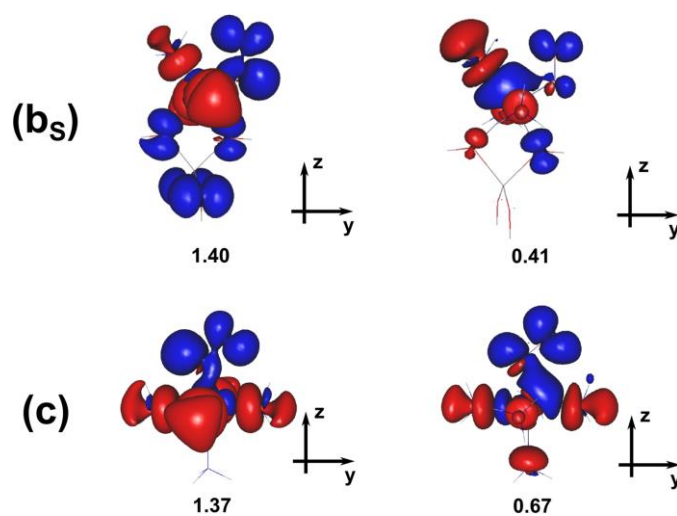


Fig.7. Dominant cumulative ($\alpha+\beta$) electron transfer channels for the singlet models (**b_S**) and (**c**) with corresponding eigenvalues (blue: accumulation, red: electron density depletion; contour value 0.001).

4. Summary and conclusions

Table 4 summarizes experimental and calculated *relative* shifts of NO stretching frequency ($\Delta\Delta_{\text{VNO}}$) in the studied systems hosting one or five ammonia ligands, with respect to NO adsorbed on a parent cationic Co(II) site in a zeolite (modeled as $[(\text{T1})\text{Co}(\text{H}_2\text{O})_2(\text{NO})]^+$). Relative shifts $\Delta\Delta_{\text{VNO}}$ calculated for the singlet or triplet ((\mathbf{b}_S) or (\mathbf{b}_T)) and the singlet (\mathbf{c}) states are listed along with the descriptor for electron transfer from the ammonia ligands to the NO (estimated from the corresponding NOCV eigenvalues). The correspondence between the relative shift of NO stretching frequency due to ammonia co-adsorption and the amount of electron density transferred from the lone pairs on NH_3 ligands to π^* antibonding orbital on NO is very good. This is especially important observation if we recall the lack of strict correlation between Δ_{VNO} and other electronic factors like the charge or spin on NO (frequently used for estimating the direction and magnitude of charge transfer).

Obviously, we do not claim that the calculated estimates of $\Delta\rho^{\text{NOCV}}_{\text{NH}_3\rightarrow\text{NO}}$ offer fully quantitative measure of charge transfer between the two types of ligands because we are aware that neither the models for Co(II) sites fully mimic properties of zeolite environment nor is the model \mathbf{c} a perfect mimic of pentaammine-coordinated Co(II)-NO, weakly bound in a zeolite framework. In addition, semi-quantitative assignment of electron-depleted or electron-enriched contours to the fragments depends on the type of the formed bond; prospective impact of the embedding (e.g. electrostatic field created by the framework) is also entirely neglected. Moreover, it must be stressed here that reliable analysis of the electron density transfer between pre-defined fragments requires as well proper selection of the non-interacting fragments as in-depth understanding of the electronic structure (e.g. spin states) of the complex containing non-innocent ligands, which not always is a routine and unarguable venture²⁸. Significant improvement in agreement when comparing *relative* experimental to

relative calculated red-shifts (taken with respect to the red-shift obtained for the Co(II) site in a pure zeolite) suggests that the influence of the environment of the cobalt cation in the adducts (modeled as either $[\text{T1Co}(\text{H}_2\text{O})_2(\text{NO})]^+$ or $[\text{T1Co}(\text{NH}_3)_n(\text{NO})]^+$) greatly cancels out (*all* calculated relative red shifts are underestimated by ca. $40\text{-}50\text{ cm}^{-1}$). The correspondence between the *relative* red-shift of NO stretching frequency (ascribed to ligation of donor ligands) and the increase of the population on the π^* antibonding orbital of NO due to additional electron density transfer from lone pairs on ammonia ligands is well featured by the designed analysis of charge transfer processes.

In general, we have shown that electron-donating ligands strongly influence the status of the site; however, the degree of their impact on the NO co-adsorbed on the same transition metal center depends dramatically as well on the spin as on the adduct type. Obviously, the type of the metal itself is also of major importance (compare cobalt to copper sites^{35,36}) but definitely, the featured electronic structure of the complex determines the final effect for cobalt. In the case of Co(II) sites with co-adsorbed ammonia, not only the number of donor co-ligands but also the spin state of the adduct appeared to be crucial for the performance of the Co(II) core (opening or closing direct channel for electron transfer). Thus the cobalt center may act as tunable electron transmitter between the co-adsorbed ligands, here electron-donating NH_3 and the target NO molecule.

Finally, the comprehensive interpretation of the region of IR spectrum attributed to ammonia-modified Co^{2+} sites in zeolites, proposed on the basis of joint IR experiment and DFT modeling, may be summarized as follows. The region corresponding to the NO stretch at $1765\text{-}1730\text{ cm}^{-1}$ may be unequivocally assigned to the triplet $\text{Co}(\text{II})(\text{NH}_3)_3(\text{NO})$ adducts. The formation of this adduct is supported by DFT calculated binding energies, indicating that substitution of two basic oxygens by NH_3 donor ligands is favored thermodynamically; the

binding energy for the third ligand is also substantial. The strongly red-shifted bands centered at 1650 cm^{-1} registered for fully ammonia-saturated zeolites are firmly attributed to $\text{Co(II)-(NH}_3)_5\text{-NO}$ adducts. Furthermore, DFT modeling offers novel interpretation for the most red-shifted band at $1600\text{-}1615\text{ cm}^{-1}$, as attributable to the singlet state of the $\text{Co(II)-(NH}_3)_3\text{-NO}$ adduct. This band shows up after NO sorption on cobalt sites after as well medium as full saturation with ammonia. This might be explained by conceivable coexistence of both spin states of the $\text{Co(II)-(NH}_3)_3\text{-NO}$ adducts after NO sorption for the intermediate saturation with ammonia and by the coexistence of all $\text{Co(II)-(NH}_3)_n\text{-NO}$ forms after NO sorption on fully ammonia-saturated zeolite. This versatility of Co(II) sites with varying activation abilities indicates that the Co(II) center acts as tunable electron donor where the spin state may open or close specific channels transferring electron density from the environment (treated as an electron reservoir) to the NO molecule.

The case study for NO adsorption on ammonia-saturated zeolites (by IR-assisted quantum chemical modeling) partly explains why the interpretation of the activity of cobalt sites in zeolites towards NO poses significant challenges and piles-up unresolved queries. We have shown that versatility of adducts, differing in geometry, electronic structure (modeling) and by the activation of NO (evidenced both by modeling and IR spectroscopy), may co-exist in zeolite frameworks. Their balance and thus the apparent activity towards NO depends on fine structural features of a particular zeolite and on experimental conditions. These aspects remain to be investigated in future studies.

Acknowledgments

The IR study was financed by Grant No. 2013/09/B/ST5/00066 from the National Science Centre, Poland. DFT modeling was funded by Grants No. 2011/01/B/ST4/02620 from the National Science Centre, Poland and by Marian Smoluchowski Krakow Research Consortium (Leading National Research Centre, KNOW).

Table 1. IR experimental N-O stretching frequencies of gaseous NO and NO in the $[\text{Co}(\text{NO})]^{2+}$ and $[\text{Co}(\text{NH}_3)_n(\text{NO})]^{2+}$ mononitrosyl complexes (re-interpreted weak features given in italics).

Zeolite	Si/Al	NO frequencies/cm ⁻¹			
		NO _{gaseous}	Co(II)-NO	[Co(II)(NH ₃) ₃]-NO	[Co(II)(NH ₃) ₅]-NO
CoFER	8.8	1875	1847	1730	<i>1615</i>
CoMOR	6.5		1852	1765, 1745	<i>1600, 1650</i>

Table 2. Selected DFT-optimized parameters relevant for NO activation (Co-N-O angle, Co-N and N-O distances) for complexes of NO with studied models of Co(II) sites: parent $[\text{T1Co}(\text{H}_2\text{O})_2]^+$ cluster and the adducts with ammonia ligands, (*available experimental values for pentaamminenitrosylcobalt(II) complex from ref. 39 in italics*).

	$[\text{T1Co}(\text{H}_2\text{O})_2(\text{NO})]^+$	$[\text{T1Co}(\text{NH}_3)_3(\text{NO})]^+$		$[\text{Co}(\text{NH}_3)_5(\text{NO})]^{2+}$
Model	(a)	(b_S)	(b_T)	(c)
$\alpha_{\text{Co-N-O}}/\text{deg}$	180	122	148	122.5 (<i>119</i>)
$d_{\text{Co-NO}}/\text{\AA}$	1.69	1.79	1.70	1.84 (<i>1.87</i>)
$d_{\text{N-O}}/\text{\AA}$	1.14	1.19	1.16	1.17 (<i>1.15</i>)

Table 3. The comparison of calculated (for all types of models) and experimental (averaged over all zeolite types) shifts of NO frequency with respect to the molecule in the gas phase; calculated charge and spin densities on NO.

Model	Interpretation	$\Delta\nu_{\text{NO}}^{\text{exp}}/\text{cm}^{-1}$ ^{a)}	$\Delta\nu_{\text{NO}}^{\text{calc}}/\text{cm}^{-1}$	Q^{NO} ^{b)}	$\rho_{\text{S}}^{\text{NO}}$ ^{b)}
(a)	Co(II)-NO	$(-7)^{\text{av}}$	+74	+0.22	0.43
(b _T)	Co(II)(NH ₃) ₃ -NO S=1	$(-109)^{\text{av}}$	-80	+0.10	0.13
(b _S)	Co(II)(NH ₃) ₃ -NO S=0	$(-250)^{\text{av}}$	-226	-0.03	0
(c)	Co(II)(NH ₃) ₅ -NO	$-(207)^{\text{av}}$ $-247^{\text{d)}$	$-166^{\text{c)}$	+0.07	0

^{a)} with respect to free NO (calc. $\nu_{\text{NO}} = 1883.56 \text{ cm}^{-1}$); ^{b)} from Mulliken population analysis; ^{c)} model completely neglecting framework embedding; ^{d)} pentaamminenitrosylcobalt(II) dichloride, after ref. 40

Table 4. Experimental and calculated relative shifts of NO stretching frequency ascribed to three or five ammonia co-ligands ($\Delta\Delta\nu_{\text{NO}}$ relative to a parent Co(II)-NO species); estimated numerical descriptors for electron transfer from ammonia ligands to NO ($\Delta\rho^{\text{NOCV}}_{\text{NH}_3\rightarrow\text{NO}}$).

Property	Three NH ₃ ligands		Five NH ₃ ligands
	Triplet	Singlet	Singlet
$\Delta\Delta\nu_{\text{NO}}^{\text{exp}}/\text{cm}^{-1}$	$(-102)^{\text{av}}$	$(-243)^{\text{av}}$	$(-200)^{\text{av}}$
$\Delta\Delta\nu_{\text{NO}}^{\text{calc}}/\text{cm}^{-1}$	-154	-290	-240
$\Delta\rho^{\text{NOCV}}_{\text{NH}_3\rightarrow\text{NO}}$	0.5	< 1.8	< 2.0

References

- ¹ Y. Traa, B. Burger, J. Weitkamp, *Micropor. Mesopor. Mater.*, 1999, 30, 3.
- ² M. Iwamoto, *Stud. Surf. Sci. Catal.*, 2000, 130A, 23.
- ³ A. E. Palomares, C. Franch, A. Corma, *Catal. Today*, 2011, 176, 239.
- ⁴ D. Pietrogiacomini, M.C. Campa, V. Indovina, *Catal. Today*, 2010, 155, 192.
- ⁵ M.C. Campa, S. De Rossi, G. Ferraris, V. Indovina, *Appl. Catal. B: Environ.*, 1996, 8, 315.
- ⁶ Y. Li, J. N. Armor, *Appl. Catal. B: Environ.*, 1993, 3, 1.
- ⁷ Y. Chang, J. G. McCarty, *J. Catal.*, 1998, 178, 408.
- ⁸ T. Montanari, O. Marie, M. Daturi, G. Busca, *Catal. Today*, 2005, 110, 339.
- ⁹ T. Grzybek, J. Klinik, M. Motak, H. Papp, *Catal. Today*, 2008, 137, 235.
- ¹⁰ Y. Li, J.N. Armor, *J. Catal.*, 1998, 176, 495.
- ¹¹ J.H. Thomas, *Adv. Chem. Ser.*, 1995, 246, 195.
- ¹² S. Bessell, *Appl. Catal.*, 1995, 126, 235.
- ¹³ K. Góra-Marek, B. Gil, J. Datka, *Appl. Catal. A: Gen.*, 2009, 353, 117.
- ¹⁴ K. Góra-Marek, H. Mrowiec, S. Walas, *J. Mol. Struct.*, 2009, 923, 67.
- ¹⁵ S. Sklenak, P.C. Andrikopoulos, S. R. Whittleton, H. Jirglova, P. Sazama, L. Benco, T. Bucko, J. Hafner, Z. Sobalik, *J. Phys. Chem. C*, 2013, 117, 3958.
- ¹⁶ T. Iizuka, J. H. Lunsford, 1978, 100, 6106.
- ¹⁷ J. H. Lunsford, P. J. Dutta, M. J. Lin, K. A. Windhorst, *Inorg. Chem.*, 1978, 17, 606.
- ¹⁸ K. A. Windhorst, J. H. Lunsford, *J. Am. Chem. Soc.*, 1975, 97, 1407.
- ¹⁹ W. B. Williamson, J. H. Lunsford, *J. Phys. Chem.*, 1976, 80, 2664.
- ²⁰ K. Góra-Marek, *Vib. Spectrosc.*, 58 (2012) 104.
- ²¹ K. Góra-Marek, J. Datka, *Catal. Today*, 2011, 169, 181.
- ²² F. Bin, C. Song, G. Lu, J. Song, X.F. Cao, H.T. Pang, K.P. Wang, *J. Phys. Chem. C*, 2012, 116, 26262.
- ²³ F. Lónyi, J. Valyon, L. Gutierrez, M.A. Ulla, E. A. Lombardo, *Appl. Catal. B: Environ.*, 73, 2007, 1.

-
- ²⁴ F. Lónyi, H. E. Solt, J. Valyon, A. Boix, L. B. Gutierrez, *Appl. Catal. B: Environ.*, 212, 2012, 117.
- ²⁵ C.J. Van Oers, K. Góra-Marek, K. Sadowska, M. Mertens, V. Meynen, J. Datka, P. Cool, *Chem. Eng. J.*, 2014, 237, 372.
- ²⁶ R. Ahlrichs, H. Horn, A. Schaefer, O. Treutler, M. Haeser, M. Baer, S. Boecker, P. Deglmann, F. Furche. *Turbomole v5.9*, Quantum Chemistry Group, Universitaet Karlsruhe, Germany, 2006.
- ²⁷ M. Radoń, E. Broclawik, K. Pierloot, *J. Phys. Chem. B*, 2010, 114, 1518.
- ²⁸ E. Broclawik, A. Stepniewski, M. Radoń, *J. Inorg. Biochem.*, 2014, 136, 147.
- ²⁹ F. Neese, *J. Biol. Inorg. Chem.*, 2006, 11, 702-711.
- ³⁰ S.A. McMillan, L.I. Broadbelt, R.Q. Snurr, *J. Catal.*, 2003, 219, 117.
- ³¹ F. Göttl, J. Hafner, *J. Chem. Phys.*, 2012, 136, 64501
- ³² F. Göttl, J. Hafner, *J. Chem. Phys.*, 2012, 136, 64502.
- ³³ F. Göttl, J. Hafner, *J. Chem. Phys.*, 2012, 136, 64503.
- ³⁴ I. Georgieva, L. Benco, D. Tunega, N. Trendafilova, J. Hafner, H. Lischka, *J. Chem. Phys.*, 2009, 131, 54101
- ³⁵ P. Kozyra, M. Radoń, J. Datka, E. Broclawik, *Struct. Chem.*, 2012, 23, 1349.
- ³⁶ M. Radoń, P. Kozyra, A. Stepniewski, J. Datka, E. Broclawik, *Can. J. Chem.*, 2013, 91, 538.
- ³⁷ M. Radoń, E. Broclawik, *J. Phys. Chem. A*, 2011, 115, 11761.
- ³⁸ J. D. Henao, L. F. Córdoba, C. M. de Correa, *J. Mol. Catal. A: Chemical*, 2004 207, 195–204
- ³⁹ C.S. Pratt, B.A. Coyle, J.A. Ibers, *J. Chem. Soc. (A)*, 1971, 2146.
- ⁴⁰ Mercer, W.A. McAllister, J.B. Durig, *Inorg. Chem.*, 1967, 6, 1816.
- ⁴¹ M. Mitoraj, A. Michalak, *J. Mol. Model*, 2007, 13, 347.
- ⁴² M. Mitoraj, A. Michalak, T. Ziegler, *J. Chem. Theory Comput.* 5 (2009) 962.
- ⁴³ S. I. Gorelsky, E. I. Solomon, *Theor Chem Account*, 2008, 119, 57–65.
- ⁴⁴ A.-R. Allouche, *J. Comp. Chem.*, 32, 2011, 174.
- ⁴⁵ M. Radoń, (2011) *Natorbs (v. 0.3)* - a universal utility for computing natural (spin)orbitals and natural orbitals for chemical valence; <http://www.chemia.uj.edu.pl/~mradon/natorbs>. Accessed July 2014.

-
- ⁴⁶ J. Dědeček, Z. Sobalík, B. Wichterlová, *Catal. Rev.: Sci. and Eng.*, 2012, 54, 135.
- ⁴⁷ R. D. Feltham and R. S. Nyholm, *Inorg. Chem.*, 1965, 4, 1334.
- ⁴⁸ R. Bruce King (Ed.), *Encyclopedia of Inorganic Chemistry*, 1994, 2, 723.
- ⁴⁹ P. Kozyra, J. Załucka, M. Mitoraj, E. Broclawik, J. Datka, *Catal. Letters*, 2008, 126, 241.
- ⁵⁰ P. Rejmak, M. Mitoraj, E. Broclawik, *Phys. Chem. Chem. Phys.*, 2010, 12, 2321.
- ⁵¹ E. Broclawik, J. Załucka, P. Kozyra, M. Mitoraj, J. Datka, *J. Phys. Chem. C*, 2010, 114, 9808.
- ⁵² E. Broclawik, M. Mitoraj, P. Rejmak and A. Michalak, *Handbook of Inorganic Chemistry Research*, D.A. Morrison (Ed), Nova Science Publishers, Inc, New York USA, 201, 1361.
- ⁵³ E. Broclawik, J. Załucka, P. Kozyra, M. Mitoraj, J. Datka, *Catal. Today*, 2011, 169, 45.
- ⁵⁴ P. Kozyra, E. Broclawik, M.P. Mitoraj, J. Datka, *J. Phys. Chem C*, 2013, 117, 7511.